
FAIR-Ensemble: When Fairness Naturally Emerges From Deep Ensembling

Wei-Yin Ko*

Cohere For AI Community

Daniel D'souza*

Cohere For AI Community

Karina Nguyen

UC Berkeley, Cohere For AI Community

Randall Balestriero

Meta AI, FAIR

Sara Hooker

Cohere For AI

Abstract

Ensembling independent deep neural networks (DNNs) is a simple and effective way to improve top-line metrics and to outperform larger single models. In this work, we go beyond top-line metrics and instead explore the impact of ensembling on subgroup performances. Surprisingly, even with a simple homogenous ensemble – all the individual models share the same training set, architecture, and design choices – we find compelling and powerful gains in worst-k and minority group performance, i.e. fairness naturally emerges from ensembling. We show that the gains in performance from ensembling for the minority group continue for far longer than for the majority group as more models are added. Our work establishes that simple DNN ensembles can be a powerful tool for alleviating disparate impact from DNN classifiers, thus curbing algorithmic harm. We also explore why this is the case. We find that even in homogeneous ensembles, varying the sources of stochasticity through parameter initialization, mini-batch sampling, and the data-augmentation realizations, results in different fairness outcomes.

1 Introduction

Deep Neural Networks (DNNs) are powerful function approximators that outperform other alternatives on a variety of tasks (Vaswani et al., 2017; Arulkumaran et al., 2017; Hinton et al., 2012; He et al., 2016b). To further boost performance, a simple and popular recipe is to average the predictions of multiple DNNs, each trained independently from the others to solve the given task, this is known as *model ensembling* (Breiman, 2001; Dietterich, 2000).

By averaging independently trained models, one avoids single model symptomatic mistakes by relying on the wisdom of the crowd to improve generalization performance, regardless of the type of model being employed. While existing work has focused on improvements to aggregate performance (Fort et al., 2019; Gupta et al., 2022; Opitz & Maclin, 1999) or gains in efficiency over a single larger model (Wang et al., 2020; Wortsman et al.,

2022), there has been limited consideration of how sensitive ensembling performance is on certain subsets of the data distribution.

Understanding performance on subgroups is frequently a concern from a fairness perspective. A common fairness objective is mitigating disparate impact (Kleinberg et al., 2016; Zafar et al., 2015) where a class or subgroup of the dataset presents far higher error rates than other subsets of the distribution. Specifically, we evaluate how ensembling impacts subgroup performance in both balanced and imbalanced settings. We evaluate the impact of ensembling on both top-k and bottom-k consisting of the K classes that the model or ensemble predicts the most and least accurately respectively, and ensemble performance on minority subgroups.

Our results are surprising: we find that while average performance quickly plateaus after a few models have been aggregated, bottom-k and minority group per-

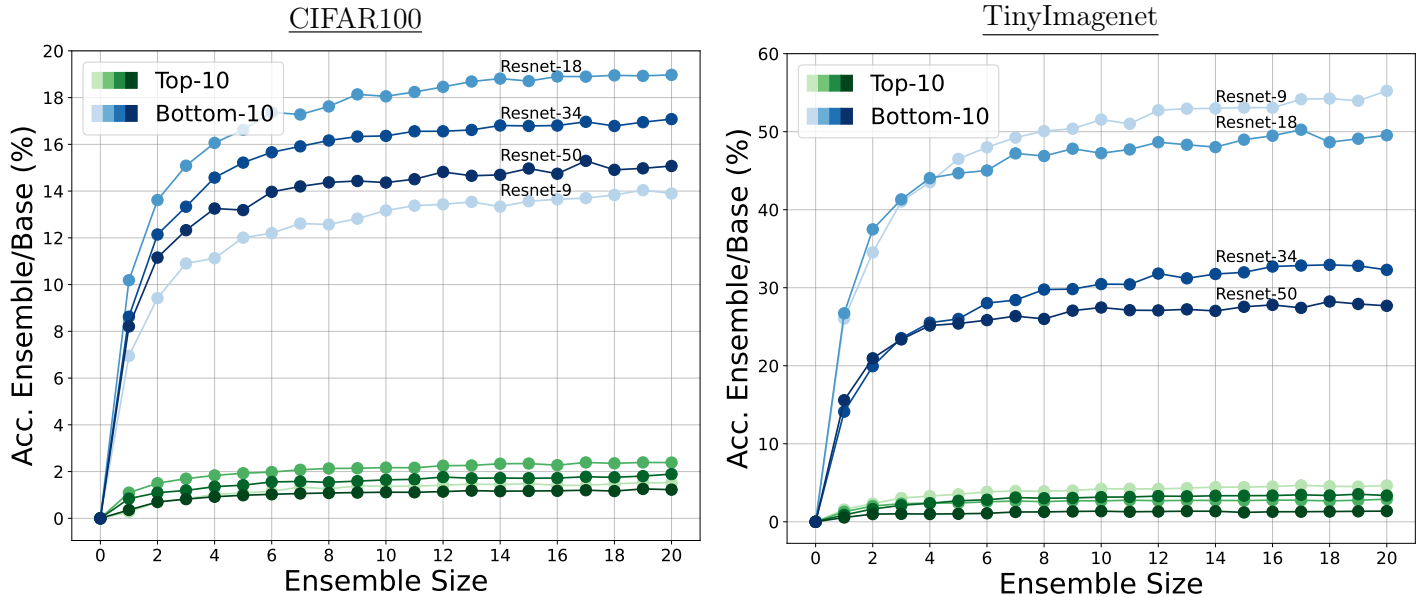


Figure 1: Relative Accuracy for Top-K/Bottom-K. Plot of the ratio of the ensemble accuracy over a single base model (y-axis) illustrates strong benefits for the minority group of ensembling (bottom-k) while the majority group (top-k) only marginally benefits.

formance disproportionately benefits from ensembling. Hence, a highly beneficial and prized property of deep ensembling with non-independent models emerges in the regime where dozens of DNNs are aggregated: improvements to fairness outcomes naturally emerge from the resulting ensemble. Furthermore, this fairness benefit appears even if all the individual models share the exact same architecture, training objective, optimization schedule and training set, i.e. the ensemble self-corrects its bias only from aggregation.

We demonstrate consistent results across thousands of experiments run on different datasets and architectures. Beyond fairness of deep ensembles, our empirical study also offers a rich variety of new observations e.g. tying the severity of image corruption to the relative benefits that emerges from deep ensembles.

Our contributions can be enumerated as follows:

1. We demonstrate that simple homogeneous deep ensembles trained with the same objective, architecture and optimization settings minimize worst-case error. This holds in both balanced and imbalanced datasets.
2. We further perform controlled sensitivity experi-

ments where constructed class imbalance and data perturbation is applied (section 4.2). We observe that homogeneous ensembles continue to improve fairness and in particular, the minority group benefits more and more as the severity of the corruption increases, while the corruption has very little impact into the majority group’s benefit from model ensembling.

3. We further dive into possible causes for this emergence of fairness in homogeneous deep ensembles by measuring model disagreement (section 5.1) and by ablating for the different sources of randomness e.g. weight-initialization (section 5.2). We obtain interesting results that suggest certain sources of stochasticity disproportionately benefit bottom-k performance.

The codebase to reproduce our results and figures is available [here](#)

2 Preliminaries

Throughout our study, we will consider a DNN to be a mapping $f_\theta : \mathcal{X} \mapsto \mathcal{Y}$ with trainable weights $\theta \in \Theta$. The training dataset \mathcal{D} consists of N data points $\mathcal{D} =$

$\{\mathbf{x}_n, y_n\}_{n=1}^N$. Given the training dataset \mathcal{D} , the trainable weights are optimized by minimizing an objective function L .

We denote an ensemble of m classification models by $\{f_{\theta_1}, \dots, f_{\theta_m}\}$, where f_{θ_i} is the i^{th} model. Each model is trained with an empirical risk minimization objective (ERM) where the goal is to minimize the average training loss.

Given n training points $\{(x_1, y_1), \dots, (x_n, y_n)\}$,

$$J_{\text{ERM}}(f_{\theta}) = \frac{1}{n} \sum_{i=1}^n \ell(x_i, y_i; f_{\theta}),$$

where $\ell(x, y; f_{\theta}) : \mathcal{X} \times \mathcal{Y} \times f_{\theta} \rightarrow \mathbb{R}_+$ is a loss function.

In our setting, each individual model is a probabilistic classifier which outputs a conditional distribution over the class labels \mathcal{Y} given the sample \mathbf{x} , i.e. $f_{\theta}(\mathbf{x}) = p(\cdot | \mathbf{x})$. Thus, for an specific data-point (\mathbf{x}, y) , the loss of an individual predictor is defined as $\ell(x, y; f_{\theta}) = -\log p(y | x, f_{\theta})$. The loss of this ensemble is defined as $\ell_{\text{ce}}(\rho, \mathbf{x}, y) = -\log \mathbb{E}_{\rho}[p(y | x, f_{\theta})]$.

In this work, we consider the impact of ensembling on both *balanced* and *imbalanced* subgroups. Fairness considerations emerge for both groups. Real world data tends to be imbalanced, where infrequent events and minority groups are less well represented in data collection processes. This leads to representational disparity (Hashimoto et al., 2018) where the under-represented group consequently experiences higher error rates. Even when training sets are balanced, with an equivalent number of training data points, certain features may be imbalanced leading to a long-tail within a balanced class. Both settings can result in *disparate impact*, where error rates for either a class or a subgroup are far higher (Chatterjee, 2020; Feldman & Zhang, 2020).

This notion of unfairness is widely documented in machine learning systems: (Buolamwini & Gebru, 2018) find that facial analysis datasets reflect a preponderance of lighter-skinned subjects, with far higher model error rates for dark skinned women. (Shankar et al., 2017) show that models trained on datasets with limited geo-diversity show sharp degradation on data drawn from other locales. Word frequency co-occurrences within

text datasets frequently reflect social biases relating to gender, race and disability (Garg et al., 2017; Zhao et al., 2018; Bolukbasi et al., 2016; Basta et al., 2019). Here, our goal is to understand whether design choices such as ensembling exacerbate or mitigate this disparity.

3 Experimental Set-up

Experimental set-up. We evaluate our methodology on CIFAR100 (Krizhevsky et al., 2009) and TinyImageNet (Russakovsky et al., 2015) datasets across various architectures: Resnet9/18/34/50 (He et al., 2016a), VGG16 (Simonyan & Zisserman, 2014) and MLP-Mixer (Tolstikhin et al., 2021), ViT (Dosovitskiy et al., 2020). We include additional training and implementation details in appendix A.

Whenever we report results on the ensemble, unless the number of models is explicitly stated, it will comprise of 20 models that were trained on the same training dataset.

All the models are trained completely independent from each other as described in (Breiman, 2001; Lee et al., 2015), i.e. we do not control for any source of randomness as this will be explored exclusively within section 5.2. With *homogeneous* training settings, the only difference between the weak learners is the inherent stochasticity introduced by DNN training. We combine the predictions from each model by averaging the predicted probabilities.

Balanced Dataset Sub-Groups. For top-k and bottom-k, we calculate the class accuracy on the base model and find the best and worst K (K=10) performing classes and track the associated images. We then proceed to measure how performance on these subgroups change as a function of the ensemble size. We highlight that although we leverage $K = 10$ to define the top and bottom groups, the precise choice of K does not impact our findings, as demonstrated in fig. 9.

Imbalanced Dataset Sub-Groups We construct a *minority* group by modifying the CIFAR10 training set to have a randomly sampled class which is only 15%, 10% of the original value. We preserve the remaining classes as balanced classes and refer to these classes as

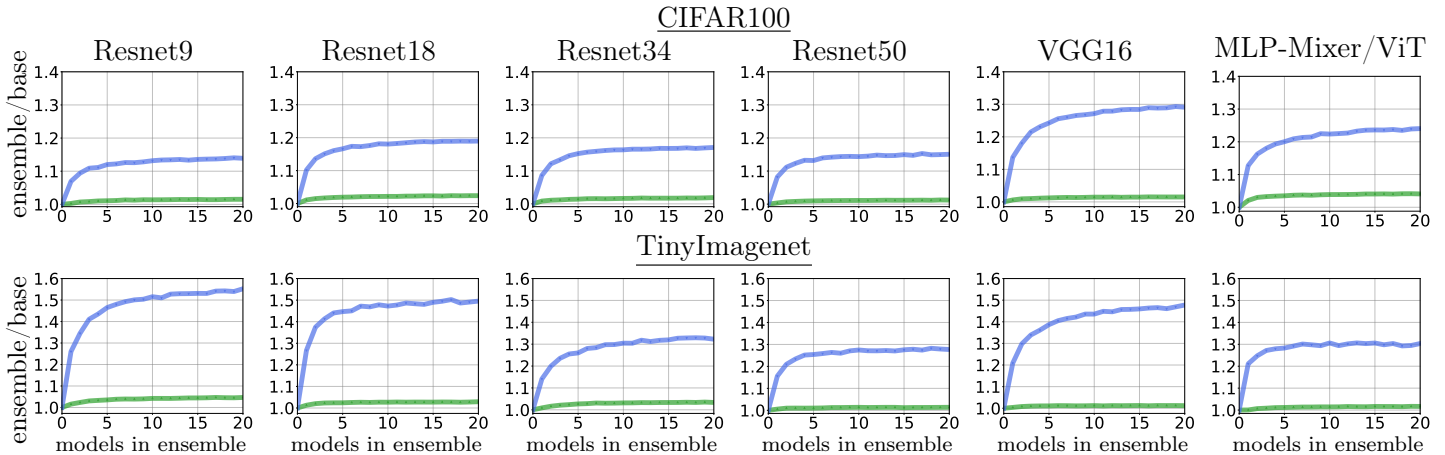


Figure 2: Depiction of the accuracy gain as a ratio of ensemble accuracy % over the singular base model (**y-axis**) by per-group (**top-k** and **bottom-k**) test set accuracies. **top row**: CIFAR100, **bottom row**: TinyImagenet. For each dataset, we plot the accuracy gain for different DNN architectures (**columns**) as the number of models within the ensemble grows (**x-axis**). We clearly observe that as the number of models within the ensemble grows, the bottom-k group benefits, i.e. its corresponding classification accuracy, outgrows the top-k group. This occurs despite the fact that the models within the ensemble are all employing the same hyperparameters-i.e. they inherently share the same functional biases. The absolute accuracies are provided in table 1 below.

majority.

4 Results and Discussion.

In (section 4.1) we establish that an ensemble of DNNs that have the same architecture and hyperparameters benefit the minority or bottom-k group. In (section 4.2) we perform a precise ablation study when controlling for class-imbalance and corruption levels in the training data, to again observe that fairness naturally emerges in deep ensembles.

4.1 Ensembling provides disproportionate gains to bottom-k and minority classes

Impact on bottom-k In fig. 1 and fig. 2, we plot the **relative gain in accuracy** i.e. the ratio between the ensemble and base model performance on top-k/bottom-k for each model architecture and dataset. This amounts to asking *what is the relative improvement in performance of using an ensemble over a single model?*

Our results are consistent across models and datasets. Ensembling disproportionately benefits bottom-k performance. For CIFAR100, this benefit ranges from 14%-

29% for bottom-k across different architectures compared to 1%-4% for top-k. For TinyImagenet the benefits are even more pronounced with a maximum gain of 55% for bottom-k compared to 5% for top-k across different architectures.

We also provide in table 1 the **absolute per-group accuracy** and average performances for the corresponding models and datasets, further reinforcing that observation. For example, we observe that a 20-model ensemble produces a maximum gain of 12.92% absolute accuracy gain for bottom-k over all architectures vs. a maximum gain of 3.86% in accuracy for top-k.

This is a crucial finding, as it demonstrates how even when ensembling DNNs that share all the same hyperparameters and trained on the same data, fairness emerges out of ensembling to improve disparate impact outcomes for bottom-k. While it is clear that bottom-k benefits the most and cannabilizes performance from top-k in some settings, the overall gains in mean accuracy indicate that often both groups benefit from ensembling with bottom-k just disproportionately so.

Impact on minority subgroups We independently train a 50 model Resnet9 ensemble on a modified cifar10 dataset with a minority and majority subgroup.

Table 1: Depiction of the average and per-group (**top-k** and **bottom-k**) absolute test set accuracies corresponding to the models and datasets depicted in fig. 2 above, again the ensemble consists of 20 models. We clearly observe that fairness naturally emerges through ensembling i.e. the bottom group substantially benefits from ensembling compared to the top group.

| Arch. | CIFAR100 | | | | | | TinyImagenet | | | | | |
|--------------|----------|-------|----------|--------|-------|----------|--------------|-------|----------|--------|-------|----------|
| | Ensemble | | | Single | | | Ensemble | | | Single | | |
| | mean | top-k | bottom-k | mean | top-k | bottom-k | mean | top-k | bottom-k | mean | top-k | bottom-k |
| Resnet9 | 77.01 | 92.18 | 58.43 | 72.21 | 90.80 | 51.30 | 58.29 | 86.66 | 23.60 | 50.71 | 82.80 | 15.20 |
| Resnet18 | 78.15 | 94.19 | 59.13 | 73.57 | 92.00 | 49.70 | 56.50 | 86.64 | 24.82 | 49.29 | 84.20 | 16.60 |
| Resnet34 | 78.68 | 93.84 | 58.89 | 74.26 | 92.10 | 50.30 | 58.89 | 87.44 | 27.25 | 52.18 | 84.60 | 20.60 |
| Resnet50 | 77.94 | 93.53 | 58.34 | 74.88 | 92.40 | 50.70 | 60.35 | 87.38 | 28.09 | 55.00 | 86.20 | 22.00 |
| VGG16 | 76.95 | 92.88 | 57.32 | 71.24 | 91.50 | 44.40 | 67.04 | 90.27 | 38.71 | 60.36 | 89.20 | 26.20 |
| MLPMixer/ViT | 66.69 | 87.95 | 40.93 | 60.25 | 84.50 | 33.00 | 56.97 | 85.60 | 22.42 | 51.23 | 84.20 | 17.20 |

In table 2, we report **average performance**, **absolute change**, **relative change** of the 50 model ensemble relative to a single base model. We observe that the minority group at both 10% and 15% benefits more than the majority from ensembling, where it receives a maximum relative gain in test-set accuracy of 9.61% vs the majority at 1.49%. We conclude that minority groups benefit the most from the average of independently trained models.

Benefits of even larger ensembles. We are interested in understanding what is an optimal number of ensembles to optimize for bottom-k gain. To do so, in fig. 2 we plot the trend lines in performance as we increase the size of the ensemble. As the number of models within the ensemble grows, accuracy gains disproportionately accrue to the bottom group versus the top group. We observe that top-k gains plateau far faster than bottom-k – indeed even at 20 model ensembles we still see positive gains for bottom-k for certain architectures such as VGG16 and Resnet9. In the appendix, we observe the limits of this trend by extending the ensemble size past 20 models; upto 50 model ensembles for some configurations in fig. 14. In both TinyImagenet and CIFAR100 datasets, the mean accuracy improvements of architectures such as Resnet9, Resnet50, and VGG16 all slowly plateaued as the ensemble reaches the size of 50. Moreover, the top-k and bottom-k relative test set accuracies of ensemble versus single model between the 20 to 50 ensemble sizes also plateaued. Continued improvements are slight to negligible as the ensemble size extends beyond 20 across all variants (as shown in figs. 15 and 16).



Figure 3: For each **row** we depict three of the different types of corruptions from the CIFAR100-C dataset (**elastic_transform**, **snow**, and **impulse_noise** respectively), and for each **column** we depict the corruption severity levels (1 \mapsto 5). The image belongs to the **lion** class.

4.2 FAIR Ensemble: Improved Robustness

Data Corruption. In this section, we aim to uncover the relationship between ensembling and performance in a corrupted inputs setting. We note that prior work has found that deep neural network ensembles improve uncertainty estimates (Lakshminarayanan et al., 2016) and can be beneficial for OOD (Xia & Bouganis, 2022). Here our goal is to instead understand how these benefits accrue to sub-groups when the data is corrupted and how this relates to the severity of the input corruption.

We benchmark our ensembles on all severity levels[1-

5] in CIFAR100-C (Hendrycks & Dietterich, 2018). CIFAR100-C is an artificially constructed dataset of 19 individual corruptions on the CIFAR100 Test Dataset. fig. 3 shows an example of the corruptions that are present in the dataset. For completeness, we benchmark and average performance across all corruptions for each severity level. In fig. 4, we plot the gain in test-set accuracy achieved by the top-k and bottom-k (K=10) classes as the ensemble size increases *relative* to a single model. We see that, consistent with earlier results, gains on top-k plateau earlier as the size of the ensemble increases. However, the benefits of ensembles are outsized when the data is noisy with corruptions. We observe in fig. 17 that the largest gains occur where there is maximum severity, with a maximum relative gain of 40.17% for severity 5 vs 20.18% for severity 1.

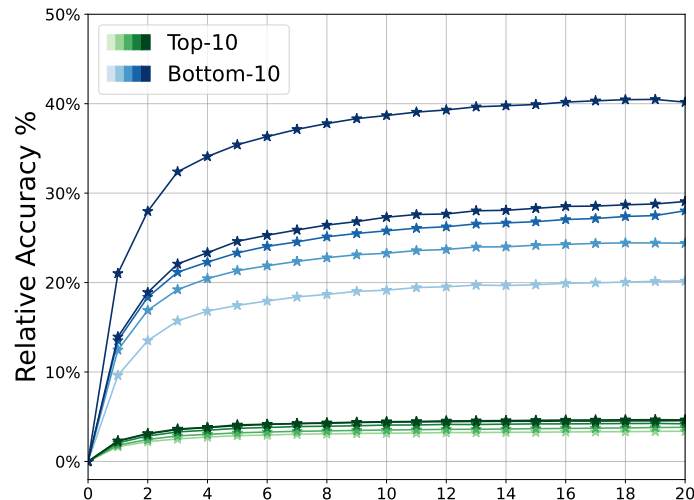


Figure 4: Depiction of the per-group (top-k and bottom-k) test performances (y-axis) of the ensemble as the number of models being aggregated increases (x-axis) and for varying severity of corruption levels (recall fig. 3) from light to dark color shading. A striking observation is that not only DNN ensembling improves fairness by increasing the performance on the bottom group more drastically than on the top group, but also that this effect is even more prominent for higher severity.

5 Why do ensembles disproportionately benefit bottom-k and minority group performance?

5.1 Difference in Churn Between Models Explains Ensemble Fairness

It might not be clear a priori how to explain the disparate impact of deep ensembling in minority groups compared to majority groups, as we observed in the previous sections 4.1 and 4.2. One popular metric of model disagreement, known as the *churn* will provide us with an obvious yet quantifiable answer which we propose to measure in this section.

Experiment set-up. To understand the benefit of model ensembling one has to recall that if all the models within the ensemble agree, then there will not be any benefit to aggregating the individual predictions. In fact, it is quite trivial to see that to aggregate the same prediction is futile. Hence, model disagreement is a key metric that will explain the stark change in performance that our DNN ensembles have shown on the minority group. We consider differences in churn between top-k and bottom-k. We also recall that the predictive churn is a measure of predictive divergence between two models. There are several different proposed definitions of predictive churn (Chen et al., 2020; Shamir & Coviello, 2020; Snapp & Shamir, 2021); we will employ the one that is defined on two models f_1 and f_2 as done by (Milani Fard et al., 2016) as the fraction of test examples where the predictions of two models disagree:

$$C(f_1, f_2) = \mathbb{E}_{\mathcal{X}} [\mathbb{1}_{\{\hat{y}_{x;f_1} \neq \hat{y}_{x;f_2}\}}], \quad (1)$$

where $\mathbb{1}$ is an indicator function for whether the predictions by each model match. For an ensemble with more than two models, we will always report the average churn computed across 100 randomly sampled (without replacement) pairwise combination of models.

Observations. In fig. 5 we report churn for each architecture we benchmark for both datasets. We observe that architectures differ in the overall level of churn, but a consistent observation across architectures is that there are large gaps in the level of churn between top-k and bottom-k. For example, on ResNet18 for TinyIm-

Table 2: Depiction of the controlled imbalanced CIFAR10 experiment for which one class (**Minority**) is subsampled to only maintain 10% (**left**) and 15% (**right**) of its original training set size, all other classes (**Majority**) are untouched. We observe again that ensembling (**All Sources row**) improves the minority group (here the sub-sampled class) much more than the majority group (the other nine classes), echoing our results from fig. 2 and table 1. We further observe that when controlling for the sources of randomness (recall section 5.3) the fairness of the ensemble can be further improved.

| variant | 10% | | | | | | 15% | | | | | |
|-------------------|---------------|--------------|-------------|-------------|-------------|-------------|---------------|--------------|-------------|-------------|-------------|-------------|
| | Ensemble Acc. | | Abs. Change | | Rel. Change | | Ensemble Acc. | | Abs. Change | | Rel. Change | |
| | Majority | Minority | Majority | Minority | Majority | Minority | Majority | Minority | Majority | Minority | Majority | Minority |
| All Sources | 95.13 | 52.95 | 1.38 | 3.45 | 1.47 | 6.97 | 95.12 | 62.72 | 1.35 | 3.02 | 1.44 | 5.06 |
| BatchOrder | 95.08 | 53.44 | 1.32 | 3.94 | 1.41 | 7.96 | 95.09 | 63.19 | 1.32 | 3.49 | 1.41 | 5.84 |
| Init | 95.03 | 52.64 | 1.27 | 3.14 | 1.36 | 6.35 | 94.97 | 62.74 | 1.21 | 3.04 | 1.29 | 5.10 |
| DA | 95.06 | 54.26 | 1.30 | 4.76 | 1.39 | 9.61 | 95.03 | 63.46 | 1.27 | 3.77 | 1.35 | 6.31 |
| Init & BatchOrder | 95.15 | 53.68 | 1.40 | 4.18 | 1.49 | 8.45 | 95.13 | 63.29 | 1.36 | 3.59 | 1.45 | 6.02 |

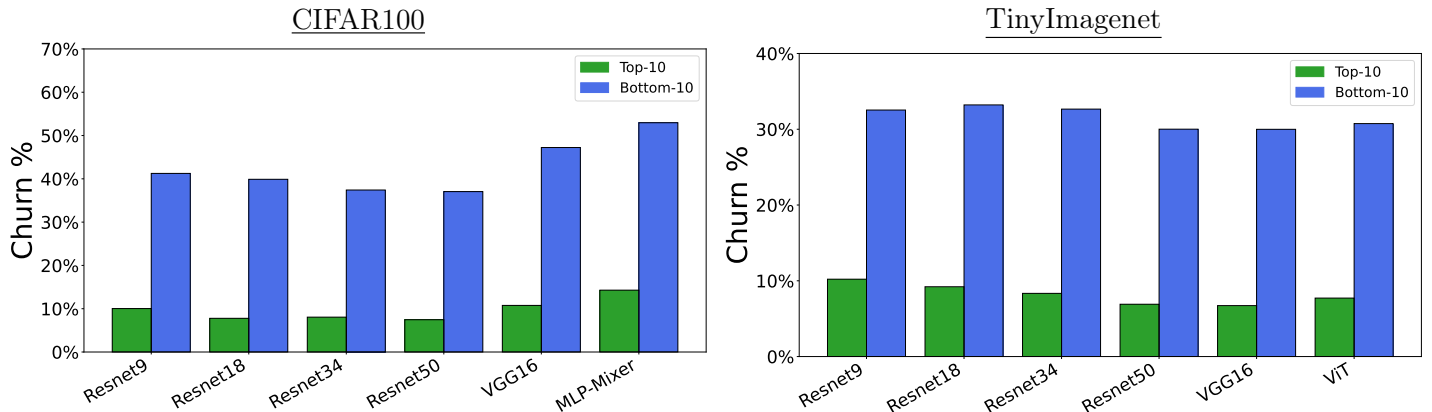


Figure 5: Depiction of churn results across models and datasets. The results demonstrate that churn is significantly higher for the **bottom-k** group compared to the **top-k** group, indicating that ensembling these models disproportionately impacts the **bottom-k** group (as defined in eq. (1)). The difference in churn between **bottom-k** and **top-k** groups varies based on model architecture, suggesting that some ensembles achieve more fairness than others.

ageNet the difference is churn of 9.22% and 33.21% for top-k and bottom-k respectively, while it is 7.78% and 39.89% for top-k and bottom-k for CIFAR100. In short, the models disagree much more when looking at samples belonging to the bottom-k groups than when looking at samples belonging to the top-k group. The models not only perform poorly on the bottom-k groups, but also vary in which samples are incorrectly classified (for definition of churn, please see eq. (1)). As a result, that group benefits much more from ensembling.

From our experience we conclude that there is not a systematic failure of a given architecture on the incorrectly classified samples (bottom-k). Furthermore, those models tend to agree on well-classified samples (top-k), where we recall that agreement is measured in

term of the churn. From those we naturally reach the observation that ensembling models is particularly useful for improving accuracy on the bottom-k samples.

5.2 Characterizing Stochasticity In Deep Neural Networks Training

What is particularly striking about our results so far is that we are observing these gains in a setting of homogeneous ensembles, where all models are trained with the same optimization choices. This means the diversity in the ensemble arises from conventional training choices that introduce stochasticity into the deep neural network optimization. Stochasticity is a crucial ingredient to produce meaningful ensembles – no stochasticity directly implies that a single model or an ensemble would be identical. In this section, we ask *why does the*

stochasticity introduced in homogenous ensembles benefit per-group performance? We study how stochasticity emerges across training from different sources (section 5.3), and also find difference in what sources of stochasticity appear to disproportionately benefit top-k vs bottom-k performance.

5.3 Controlling for the Sources of Stochasticity in Ensembles

To understand more what introduces the most significant levels of stochasticity, we first explore how different sources of randomness impact the training trajectories of DNNs. Deep Neural Network training includes model design choices which are inherently stochastic, including implementation choices such as *Random Initialization* (Glorot & Bengio, 2010; He et al., 2016b), *Data augmentation* (Kukačka et al., 2017; Hernández-García & König, 2018), *Data shuffling and ordering* (Smith et al., 2018; Shumailov et al., 2021). In this section we ask *What source dominates stochasticity in DNN training? Can we perform ablations to understand whether there are more beneficial distributions of stochasticity for fairness outcomes?*

Experiment set-up. To isolate the impact of the different sources of stochasticity, we propose a thorough ablation study. In particular, we consider the following sources:

- **Change Model Initialization (Init):** for this ablation, we change the model initialization weights by changing the torch seed for each model before the model is instantiated.
- **Change Batch Ordering (BatchOrder):** for this ablation, we change the ordering of image data in each minibatch by changing the seed for the dataloader for each model training.
- **Change Model Initialization and Batch Ordering (Init & BatchOrder):** for this ablation, both the model initialization and batch ordering are changed for each model training.
- **Change Data Augmentation (DA):** for this ablation, only the randomness in the data augmentation (e.g. probability of random flips, probability of CutMix(Yun et al., 2019), etc.) is changed.

The relevant torch and numpy seeds are changed right before instantiating the data augmentation pipeline. Custom fixed-seed data augmentations is also used.

- **Change Model Initialization, Batch Ordering and Data Augmentation (All Sources):** for this ablation, the model initialization, batch ordering and data augmentation seeds are changed for each model training. This ablation is used as the baseline to compare with the other ablations.

A last source of randomness can emerge from hardware or software choices and round-off errors (Zhuang et al., 2022; Shallue et al., 2019) which we found to be negligible compared to the others, and as we use the exact same hardware and software choices across experiments, we already control for it and thus omit it from our study. In order to measure the amount of stochasticity that each of the above sources accounts for we will not only visually depict the per-group performances between individual training episodes, but we also propose the use of two quantitative metrics. First, we will leverage the **L1-Distance** which is calculated for every epoch by averaging the absolute distance in accuracy among the ensemble members. The final metric is obtained by averaging these values across the training epochs. We will also leverage the **Variance** which is calculated on the accuracy among the ensemble members at a given epoch. The final metric is obtained by averaging these values across the training epochs.

Observations. In fig. 6, we plot these measures of stochasticity for both CIFAR100 and TinyImagenet on different networks. We observe that the single sources of noise dominate, such that the ablations themselves equate to the level of noise in the network with all sources of noise present. In particular, we observe one striking phenomenon: the variation of the data ordering within each epoch between training trajectories **BatchOrder** is the main source of randomness. It is equivalent to the level of noise we observe for the network with all sources of noise **All Sources**, and the network with the ablation **Init & BatchOrder**. As seen in fig. 6 when the batch-ordering is kept the same across training episodes, varying the data-augmentation and/or the model initialization has very little impact.

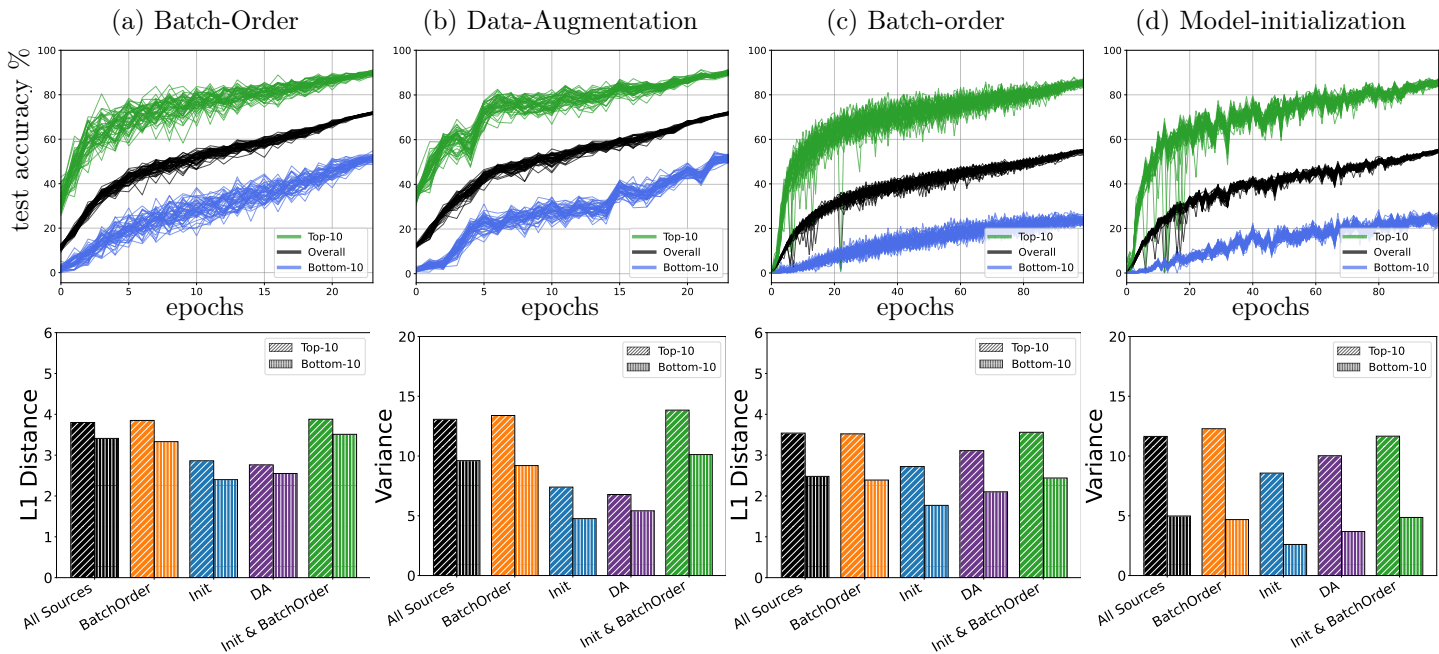


Figure 6: Depiction of multiple individual training episodes of a Resnet9 model on CIFAR100 (top row, left) and Resnet50 model on TinyImagenet (top row, right). We clearly observe that varying one factor of stochasticity at a time highlights which ones provide the most randomness between training episodes, in particular in this setting we see that batch-ordering is the main source. On the other hand model-init and data-augmentation have little effect and we even observe very similar trends at different epochs between the individual runs.

5.4 Can Different Sources of Stochasticity Improve Deep Ensemble Fairness?

We already observed that standard ensembles, i.e. with no source of stochasticity being controlled, improve fairness over individual models (recall sections 4.1 and 4.2). Yet, we also observed in the previous section 5.3 that different sources of stochasticity have a clear impact into individual training episodes of a DNN. In this section, we seek to understand how these different sources of noise aggregate in an ensemble and the differences in fairness outcomes these sources of noise produce. We also seek to understand if certain distributions of noise benefit top-k versus bottom-k performance.

Dominant sources of stochasticity. In fig. 7, we plot the **accuracy difference** between average top-k and bottom-k. At 0 this measure indicates that the model performs uniformly on both top-k and bottom-k. We observe that for the majority of dataset/architecture combinations, batch-ordering minimizes the gap be-

tween top and bottom-k class accuracy. There is one exception to this, as we see that data-augmentation variation for Resnet18 on TinyImagenet creates the largest decrease.

Distributions of Stochasticity that benefit majority vs minority. While **accuracy difference** gives a sense of what bridges the gap between sub-group performance, it does not tell us if certain sources of noise benefit minority subgroups more. To understand this, we compare our noise ablations of our minority group experiment in section 4.2. In table 2, we see a consistent trend, where stochasticity introduced by data augmentation DA consistently favors minority group performance, and stochasticity introduced by initialization and batch ordering Init & BatchOrder consistently favors majority group performance.

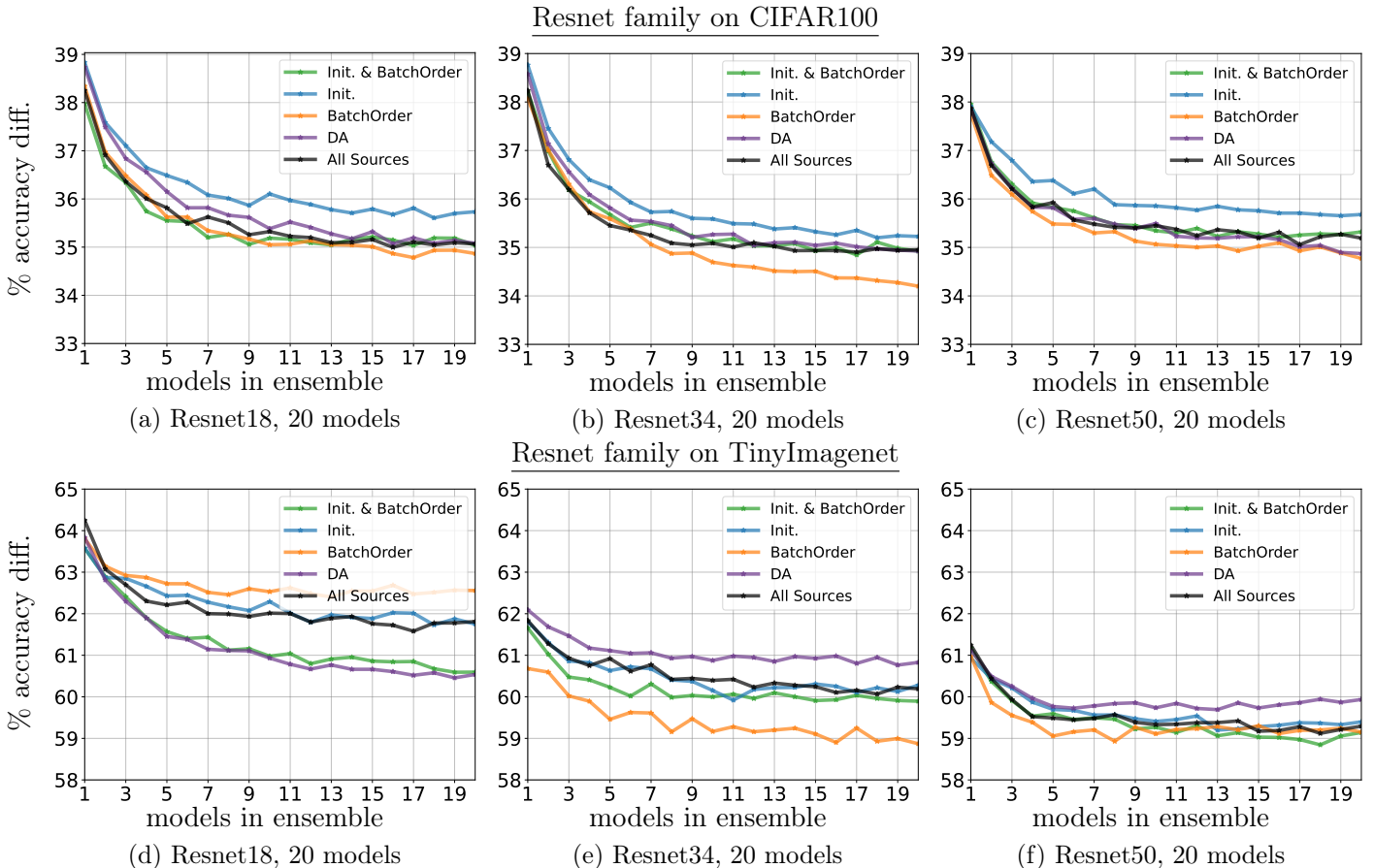


Figure 7: Accuracy % difference between top and bottom 10 classes, for Resnet18, 34, and 50 for CIFAR100 and TinyImagenet. We clearly observe that once we control for the different sources of stochasticities, it is possible to skew the ensemble to favor the bottom group, in which case fairness is further amplified compared to the baseline ensemble, but also to favor the top group, in which case fairness is worse than the baseline ensemble. Although the trends seem mostly consistent across architectures of the same family (Resnets) and datasets, it is not necessarily the case between architecture families: see fig. 10 for additional runs on CIFAR100 with MLP-Mixer and VGG16, and on TinyImagenet with VGG16 and ViT.

6 Related Work

Deep ensembling of neural networks has been shown to be a simple and popular formula for improving top-line metrics (Lakshminarayanan et al., 2016). Several works have sought to further improve aggregate performance by amplifying differences between models in the ensemble – ranging from varying the data augmentation used for each model (Stickland & Murray, 2020), architecture (Zaidi et al., 2021), and hyperparameters (Wortsmann et al., 2022) to objectives (Jain et al., 2020). In contrast to prior work, we focus on simple ensembles where all design choices are shared between each model in the ensemble. We are also focused on understanding the implications of ensembling on fairness objectives, rather than on top-line metrics.

Beyond Top-line metrics Discussions of algorithmic bias often focus on the way in which our datasets are collected and curated (Barocas et al., 2019; Zhao et al., 2017; Shankar et al., 2017), with limited work to-date understanding the role of model design or optimization choices on amplifying or curbing bias (Ogueji et al., 2022; Hooker et al., 2019). Consistent with this, there has been limited work to-date on understanding the implications of ensembling on subgroup error. (Grgić-Hlača et al., 2017) point out the theoretical possibility of using an ensemble to improve model fairness on a simple binary model. However, they do not provide empirical evidence and limit consideration to an ensemble formed by randomly selecting the individual models from a set of possible classifiers. In contrast, our work establishes that ensembles mitigate harm across 1000s of

model and dataset combinations. Another relevant work is (Bhaskaruni et al., 2019) which considers AdaBoost (Freund & Schapire, 1995) ensembles and shows that upweighting unfairly predicted examples reaches higher fairness when learning base models. In contrast to our simple averaging of predictions of homogeneous DNNs trained in parallel, the authors explicitly optimize for improved fairness by using boosting techniques with a focus on specialized ensembles.

Understanding why ensembling benefits subgroup performance. Several works to date have sought to understand why weight averaging performs well and improves top-line metrics (Gupta et al., 2022). However, few to our knowledge have sought to understand why ensembles disproportionately benefit bottom-k and minority group performance. (Rame et al., 2022) explore why weight averaging performs well on out-of-distribution data, relating variance to diversity shift. In this work, we instead explore how individual sources of inherent stochasticity in uniform ensembles impact subgroup performance.

Impact of stochasticity on fairness objectives Several works to-date have considered how stochasticity can impact top-line metrics (Nagarajan et al., 2018). Most relevant to our work is (Qian et al., 2021; Zhuang et al., 2022; Madhyastha & Jain, 2019; Summers & Dinneen, 2021) that evaluates how stochasticity in training impacts fairness in DNN Systems. However, all these works restrict their treatment to a single model setting, and do not evaluate the impact of ensembling.

7 Conclusion and Future Work

In this work, we establish that while ensembling is often seen as a method of improving average performance, it can also provide significant fairness gains. This suggests ensembles are a powerful tool to improve fairness outcomes in sensitive domains where human welfare is at risk. We explore why ensembles are so effective at improving fairness outcomes, and find that certain distributions of stochasticity appear to disproportionately favor top-k and bottom-k. This is an interesting avenue of future work, and suggests designing ensembles which amplify certain sources of stochasticity may further amplify the gains for fairness outcomes.

Future work. Our work ablating sources of stochasticity and finding that certain sources consistently favor minority and majority groups suggests that future work should explicitly optimize to amplify these sources. Another avenue would be to a priori identify, given an architecture, the source of stochasticity that will favor fairness. We obtained preliminary results that such sources might vary based on the architecture.

References

- Kai Arulkumaran, Marc Peter Deisenroth, Miles Brundage, and Anil Anthony Bharath. A brief survey of deep reinforcement learning. *arXiv preprint arXiv:1708.05866*, 2017.
- Solon Barocas, Moritz Hardt, and Arvind Narayanan. *Fairness and Machine Learning: Limitations and Opportunities*. fairmlbook.org, 2019. <http://www.fairmlbook.org>.
- Christine Basta, Marta R. Costa-jussà, and Noe Casas. Evaluating the underlying gender bias in contextualized word embeddings. In *Proceedings of the First Workshop on Gender Bias in Natural Language Processing*, pp. 33–39, Florence, Italy, August 2019. Association for Computational Linguistics. doi: 10.18653/v1/W19-3805. URL <https://aclanthology.org/W19-3805>.
- Dheeraj Bhaskaruni, Hui Hu, and Chao Lan. Improving prediction fairness via model ensemble. In *2019 IEEE 31st International Conference on Tools with Artificial Intelligence (ICTAI)*, pp. 1810–1814, 2019. doi: 10.1109/ICTAI.2019.00273.
- Tolga Bolukbasi, Kai-Wei Chang, James Y Zou, Venkatesh Saligrama, and Adam T Kalai. Man is to computer programmer as woman is to homemaker? debiasing word embeddings. *Advances in neural information processing systems*, 29, 2016.
- Leo Breiman. Random forests. *Machine learning*, 45(1):5–32, 2001.
- Joy Buolamwini and Timnit Gebru. Gender shades: Intersectional accuracy disparities in commercial gender classification. In *Conference on fairness, accountability and transparency*, pp. 77–91, 2018.
- Satrajit Chatterjee. Coherent gradients: An approach to understanding generalization in gradient descent-based optimization. *arXiv preprint arXiv:2002.10657*, 2020.
- Zhe Chen, Yuyan Wang, Dong Lin, Derek Zhiyuan Cheng, Lichan Hong, Ed H. Chi, and Claire Cui. Beyond point estimate: Inferring ensemble prediction variation from neuron activation strength in recommender systems, 2020.
- Ekin D Cubuk, Barret Zoph, Dandelion Mane, Vijay Vasudevan, and Quoc V Le. Autoaugment: Learning augmentation policies from data. *arXiv preprint arXiv:1805.09501*, 2018.
- Thomas G Dietterich. Ensemble methods in machine learning. In *International workshop on multiple classifier systems*, pp. 1–15. Springer, 2000.
- Alexey Dosovitskiy, Lucas Beyer, Alexander Kolesnikov, Dirk Weissenborn, Xiaohua Zhai, Thomas Unterthiner, Mostafa Dehghani, Matthias Minderer, Georg Heigold, Sylvain Gelly, et al. An image is worth 16x16 words: Transformers for image recognition at scale. *arXiv preprint arXiv:2010.11929*, 2020.
- Vitaly Feldman and Chiyuan Zhang. What neural networks memorize and why: Discovering the long tail via influence estimation. In H. Larochelle, M. Ranzato, R. Hadsell, M. F. Balcan, and H. Lin (eds.), *Advances in Neural Information Processing Systems*, volume 33, pp. 2881–2891. Curran Associates, Inc., 2020. URL <https://proceedings.neurips.cc/paper/2020/file/1e14bfe2714193e7af5abc64ecbd6b46-Paper.pdf>.
- Stanislav Fort, Huiyi Hu, and Balaji Lakshminarayanan. Deep ensembles: A loss landscape perspective. *arXiv preprint arXiv:1912.02757*, 2019.
- Yoav Freund and Robert E. Schapire. A decision-theoretic generalization of on-line learning and an application to boosting. In *EuroCOLT*, 1995.
- Nikhil Garg, Londa Schiebinger, Dan Jurafsky, and James Zou. Word embeddings quantify 100 years of gender and ethnic stereotypes. *Proceedings of the National Academy of Sciences*, 115, 11 2017. doi: 10.1073/pnas.1720347115.
- Xavier Glorot and Yoshua Bengio. Understanding the difficulty of training deep feedforward neural networks. In Yee Whye Teh and Mike Titterton (eds.), *Proceedings of the Thirteenth International Conference on Artificial Intelligence and Statistics*, volume 9 of *Proceedings of Machine Learning Research*, pp. 249–256, Chia Laguna Resort, Sardinia, Italy, 13–15 May 2010. PMLR. URL <http://proceedings.mlr.press/v9/glorot10a.html>.

-
- Nina Grgić-Hlača, Muhammad Bilal Zafar, Krishna P. Gummadi, and Adrian Weller. On fairness, diversity and randomness in algorithmic decision making, 2017. URL <https://arxiv.org/abs/1706.10208>.
- Neha Gupta, Jamie Smith, Ben Adlam, and Zelda Mariet. Ensembling over classifiers: a bias-variance perspective. *arXiv preprint arXiv:2206.10566*, 2022.
- Tatsunori Hashimoto, Megha Srivastava, Hongseok Namkoong, and Percy Liang. Fairness without demographics in repeated loss minimization. In Jennifer Dy and Andreas Krause (eds.), *Proceedings of the 35th International Conference on Machine Learning*, volume 80 of *Proceedings of Machine Learning Research*, pp. 1929–1938, Stockholmsmässan, Stockholm Sweden, 10–15 Jul 2018. PMLR. URL <http://proceedings.mlr.press/v80/hashimoto18a.html>.
- Kaiming He, Xiangyu Zhang, Shaoqing Ren, and Jian Sun. Deep residual learning for image recognition. In *CVPR*, 2016a.
- Kaiming He, Xiangyu Zhang, Shaoqing Ren, and Jian Sun. Deep residual learning for image recognition. In *2016 IEEE Conference on Computer Vision and Pattern Recognition, CVPR*, 2016b.
- Dan Hendrycks and Thomas G Dietterich. Benchmarking neural network robustness to common corruptions and surface variations. *arXiv preprint arXiv:1807.01697*, 2018.
- Alex Hernández-García and Peter König. Further advantages of data augmentation on convolutional neural networks. *Lecture Notes in Computer Science*, pp. 95–103, 2018. ISSN 1611-3349. doi: 10.1007/978-3-030-01418-6_10. URL http://dx.doi.org/10.1007/978-3-030-01418-6_10.
- Geoffrey Hinton, Li Deng, Dong Yu, George E Dahl, Abdel-rahman Mohamed, Navdeep Jaitly, Andrew Senior, Vincent Vanhoucke, Patrick Nguyen, Tara N Sainath, et al. Deep neural networks for acoustic modeling in speech recognition: The shared views of four research groups. *IEEE Signal processing magazine*, 29(6):82–97, 2012.
- Sara Hooker, Aaron Courville, Gregory Clark, Yann Dauphin, and Andrea Frome. What Do Compressed Deep Neural Networks Forget? *arXiv e-prints*, art. arXiv:1911.05248, November 2019.
- Jeremy Howard and Sebastian Ruder. Universal language model fine-tuning for text classification. *arXiv preprint arXiv:1801.06146*, 2018.
- Siddhartha Jain, Ge Liu, Jonas Mueller, and David Gifford. Maximizing overall diversity for improved uncertainty estimates in deep ensembles. In *Proceedings of the AAAI Conference on Artificial Intelligence*, volume 34, pp. 4264–4271, 2020.
- Diederik P Kingma and Jimmy Ba. Adam: A method for stochastic optimization. *arXiv preprint arXiv:1412.6980*, 2014.
- Jon M. Kleinberg, Sendhil Mullainathan, and Manish Raghavan. Inherent trade-offs in the fair determination of risk scores. *CoRR*, abs/1609.05807, 2016. URL <http://arxiv.org/abs/1609.05807>.
- Alex Krizhevsky, Geoffrey Hinton, et al. Learning multiple layers of features from tiny images. 2009.
- Jan Kukačka, Vladimir Golkov, and Daniel Cremers. Regularization for deep learning: A taxonomy, 2017.
- Balaji Lakshminarayanan, Alexander Pritzel, and Charles Blundell. Simple and Scalable Predictive Uncertainty Estimation using Deep Ensembles. *arXiv e-prints*, art. arXiv:1612.01474, Dec 2016.
- Stefan Lee, Senthil Purushwalkam, Michael Cogswell, David J. Crandall, and Dhruv Batra. Why M heads are better than one: Training a diverse ensemble of deep networks. *CoRR*, abs/1511.06314, 2015. URL <http://arxiv.org/abs/1511.06314>.
- Ilya Loshchilov and Frank Hutter. Sgdr: Stochastic gradient descent with warm restarts. *arXiv preprint arXiv:1608.03983*, 2016.
- Ilya Loshchilov and Frank Hutter. Decoupled weight decay regularization. *arXiv preprint arXiv:1711.05101*, 2017.
- Pranava Madhyastha and Rishabh Jain. On model stability as a function of random seed. *arXiv preprint arXiv:1909.10447*, 2019.

-
- Mahdi Milani Fard, Quentin Cormier, Kevin Canini, and Maya Gupta. Launch and iterate: Reducing prediction churn. In D. Lee, M. Sugiyama, U. Luxburg, I. Guyon, and R. Garnett (eds.), *Advances in Neural Information Processing Systems*, volume 29. Curran Associates, Inc., 2016. URL <https://proceedings.neurips.cc/paper/2016/file/dc5c768b5dc76a084531934b34601977-Paper.pdf>.
- Prabhat Nagarajan, Garrett Warnell, and Peter Stone. The impact of nondeterminism on reproducibility in deep reinforcement learning. In *Reproducibility in ML Workshop at the 35th International Conference on Machine Learning, ICML*, 2018.
- Kelechi Ogueji, Orevaoghene Ahia, Gbemileke Onilude, Sebastian Gehrmann, Sara Hooker, and Julia Kreutzer. Intriguing properties of compression on multilingual models, 2022. URL <https://arxiv.org/abs/2211.02738>.
- D. Opitz and R. Maclin. Popular ensemble methods: An empirical study. *Journal of Artificial Intelligence Research*, 11:169–198, aug 1999. doi: 10.1613/jair.614. URL <https://doi.org/10.1613%2Fjair.614>.
- Shangshu Qian, Viet Hung Pham, Thibaud Lutellier, Zeou Hu, Jungwon Kim, Lin Tan, Yaoliang Yu, Jiahao Chen, and Sameena Shah. Are my deep learning systems fair? an empirical study of fixed-seed training. *Advances in Neural Information Processing Systems*, 34:30211–30227, 2021.
- Alexandre Rame, Matthieu Kirchmeyer, Thibaud Rahier, Alain Rakotomamonjy, Patrick Gallinari, and Matthieu Cord. Diverse weight averaging for out-of-distribution generalization. *arXiv preprint arXiv:2205.09739*, 2022.
- Olga Russakovsky, Jia Deng, Hao Su, Jonathan Krause, Sanjeev Satheesh, Sean Ma, Zhiheng Huang, Andrej Karpathy, Aditya Khosla, Michael Bernstein, et al. Imagenet large scale visual recognition challenge. In *IJCV*, 2015.
- Christopher J. Shallue, Jaehoon Lee, Joseph Antognini, Jascha Sohl-Dickstein, Roy Frostig, and George E. Dahl. Measuring the effects of data parallelism on neural network training, 2019.
- Gil I. Shamir and Lorenzo Coviello. Anti-distillation: Improving reproducibility of deep networks. *CoRR*, abs/2010.09923, 2020. URL <https://arxiv.org/abs/2010.09923>.
- Shreya Shankar, Yoni Halpern, Eric Breck, James Atwood, Jimbo Wilson, and D Sculley. No classification without representation: Assessing geodiversity issues in open data sets for the developing world. *arXiv preprint arXiv:1711.08536*, 2017.
- Ilya Shumailov, Zakhar Shumaylov, Dmitry Kazhdan, Yiren Zhao, Nicolas Papernot, Murat A. Erdogdu, and Ross Anderson. Manipulating sgd with data ordering attacks, 2021.
- Karen Simonyan and Andrew Zisserman. Very deep convolutional networks for large-scale image recognition. *arXiv preprint arXiv:1409.1556*, 2014.
- Samuel L. Smith, Pieter-Jan Kindermans, Chris Ying, and Quoc V. Le. Don’t decay the learning rate, increase the batch size, 2018.
- Robert R. Snapp and Gil I. Shamir. Synthesizing irreproducibility in deep networks. *CoRR*, abs/2102.10696, 2021. URL <https://arxiv.org/abs/2102.10696>.
- Asa Cooper Stickland and Iain Murray. Diverse ensembles improve calibration. *CoRR*, abs/2007.04206, 2020. URL <https://arxiv.org/abs/2007.04206>.
- Cecilia Summers and Michael J Dinneen. Nondeterminism and instability in neural network optimization. In *International Conference on Machine Learning*, pp. 9913–9922. PMLR, 2021.
- Ilya O Tolstikhin, Neil Houlsby, Alexander Kolesnikov, Lucas Beyer, Xiaohua Zhai, Thomas Unterthiner, Jessica Yung, Andreas Steiner, Daniel Keysers, Jakob Uszkoreit, et al. Mlp-mixer: An all-mlp architecture for vision. *Advances in Neural Information Processing Systems*, 34:24261–24272, 2021.
- Ashish Vaswani, Noam Shazeer, Niki Parmar, Jakob Uszkoreit, Llion Jones, Aidan N. Gomez, Lukasz Kaiser, and Illia Polosukhin. Attention is All you Need. In *Advances in Neural Information Processing Systems 30: Annual Conference on Neural Information Processing Systems 2017, 4-9 December 2017, Long Beach, CA, USA*, pp. 6000–6010, 2017.

-
- Xiaofang Wang, Dan Kondratyuk, Kris M. Kitani, Yair Movshovitz-Attias, and Elad Eban. Multiple networks are more efficient than one: Fast and accurate models via ensembles and cascades. *CoRR*, abs/2012.01988, 2020. URL <https://arxiv.org/abs/2012.01988>.
- Mitchell Wortsman, Gabriel Ilharco, Samir Ya Gadre, Rebecca Roelofs, Raphael Gontijo-Lopes, Ari S Morcos, Hongseok Namkoong, Ali Farhadi, Yair Carmon, Simon Kornblith, et al. Model soups: averaging weights of multiple fine-tuned models improves accuracy without increasing inference time. In *International Conference on Machine Learning*, pp. 23965–23998. PMLR, 2022.
- Guoxuan Xia and Christos-Savvas Bouganis. On the usefulness of deep ensemble diversity for out-of-distribution detection. *arXiv preprint arXiv:2207.07517*, 2022.
- Sangdoon Yun, Dongyoon Han, Seong Joon Oh, Sanghyuk Chun, Junsuk Choe, and Youngjoon Yoo. Cutmix: Regularization strategy to train strong classifiers with localizable features. In *Proceedings of the IEEE/CVF international conference on computer vision*, pp. 6023–6032, 2019.
- Muhammad Bilal Zafar, Isabel Valera, Manuel Gomez Rodriguez, and Krishna P. Gummadi. Fairness constraints: Mechanisms for fair classification, 2015. URL <https://arxiv.org/abs/1507.05259>.
- Sheheryar Zaidi, Arber Zela, Thomas Elsken, Chris C Holmes, Frank Hutter, and Yee Teh. Neural ensemble search for uncertainty estimation and dataset shift. *Advances in Neural Information Processing Systems*, 34:7898–7911, 2021.
- Hongyi Zhang, Moustapha Cisse, Yann N Dauphin, and David Lopez-Paz. mixup: Beyond empirical risk minimization. *arXiv preprint arXiv:1710.09412*, 2017.
- Jieyu Zhao, Tianlu Wang, Mark Yatskar, Vicente Ordonez, and Kai-Wei Chang. Men also like shopping: Reducing gender bias amplification using corpus-level constraints. In *Proceedings of the 2017 Conference on Empirical Methods in Natural Language Processing*, September 2017.
- Jieyu Zhao, Tianlu Wang, Mark Yatskar, Vicente Ordonez, and Kai-Wei Chang. Gender bias in coreference resolution: Evaluation and debiasing methods. In *Proceedings of the 2018 Conference of the North American Chapter of the Association for Computational Linguistics: Human Language Technologies, Volume 2 (Short Papers)*, pp. 15–20, New Orleans, Louisiana, June 2018. Association for Computational Linguistics. doi: 10.18653/v1/N18-2003. URL <https://aclanthology.org/N18-2003>.
- Zhun Zhong, Liang Zheng, Guoliang Kang, Shaozi Li, and Yi Yang. Random erasing data augmentation. In *Proceedings of the AAAI conference on artificial intelligence*, volume 34, pp. 13001–13008, 2020.
- Donglin Zhuang, Xingyao Zhang, Shuaiwen Song, and Sara Hooker. Randomness in neural network training: Characterizing the impact of tooling. In D. Marculescu, Y. Chi, and C. Wu (eds.), *Proceedings of Machine Learning and Systems*, volume 4, pp. 316–336, 2022. URL <https://proceedings.mlsys.org/paper/2022/file/757b505cfd34c64c85ca5b5690ee5293-Paper.pdf>.

A Experimental Setup

A.1 Sampling

Given a pool of M models, for each ensemble size S we sample 100 times with replacement. We then average the accuracy across the 100 samples plus one base model that is shared across all variants. The results at each S is reported until an ensemble of M models is reached.

A.2 CIFAR-100 Training

We use the following architectures: Resnet9 (He et al., 2016a), VGG16 (Simonyan & Zisserman, 2014) and MLP-Mixer (Tolstikhin et al., 2021). We train them as follows :

Resnet-9 We train the model for 24 steps using Stochastic Gradient Descent (SGD). We implemented standard data augmentation by applying Random Horizontal Flip, Random Translate, and Cutout. We use a Slanted Triangular Learning Rate (SLTR) (Howard & Ruder, 2018). The top-1 test set accuracy is 72.24%

Resnet18/34/50 For these 3 Resnet architectures, we train the model for 50 epochs using Stochastic Gradient Descent (SGD), batch size of 512, momentum=0.9, and weight decay=0.0005. We implemented standard data augmentation by applying Random Horizontal Flip, Random Crop, Random Affine, and Cutout. We use a combination of warmup for first 5 epoch and cosine annealing for scheduler. The top-1 test set accuracy for Resnet-18 is 73.56%, Resnet-34 is 74.24%, and Resnet-50 is 74.89%

VGG16 We train the model for 130 epochs using Stochastic Gradient Descent (SGD). We implemented standard data augmentation by applying Random Horizontal Flip, Random Crop, and Random Rotation. We use a combination of warmup for 1 epoch and a multi-step scheduler with milestones at steps 60 and 120. The top-1 test set accuracy is 71.23%

MLP-Mixer We train the model for 300 steps using Adaptive Moment Estimation (Adam) (Kingma & Ba, 2014). We implemented standard data augmentation by applying Random Crop, AutoAugment (CIFAR10 Policy) (Cubuk et al., 2018), and CutMix (Yun et al., 2019). We use a combination of warmup for first 5 epoch and cosine annealing for scheduler. The top-1 test set accuracy is 60.28%

A.3 TinyImageNet Training

We use the following architectures: Resnets (He et al., 2016a), VGG-16 (Simonyan & Zisserman, 2014) and ViT (Dosovitskiy et al., 2020). We train them as follows :

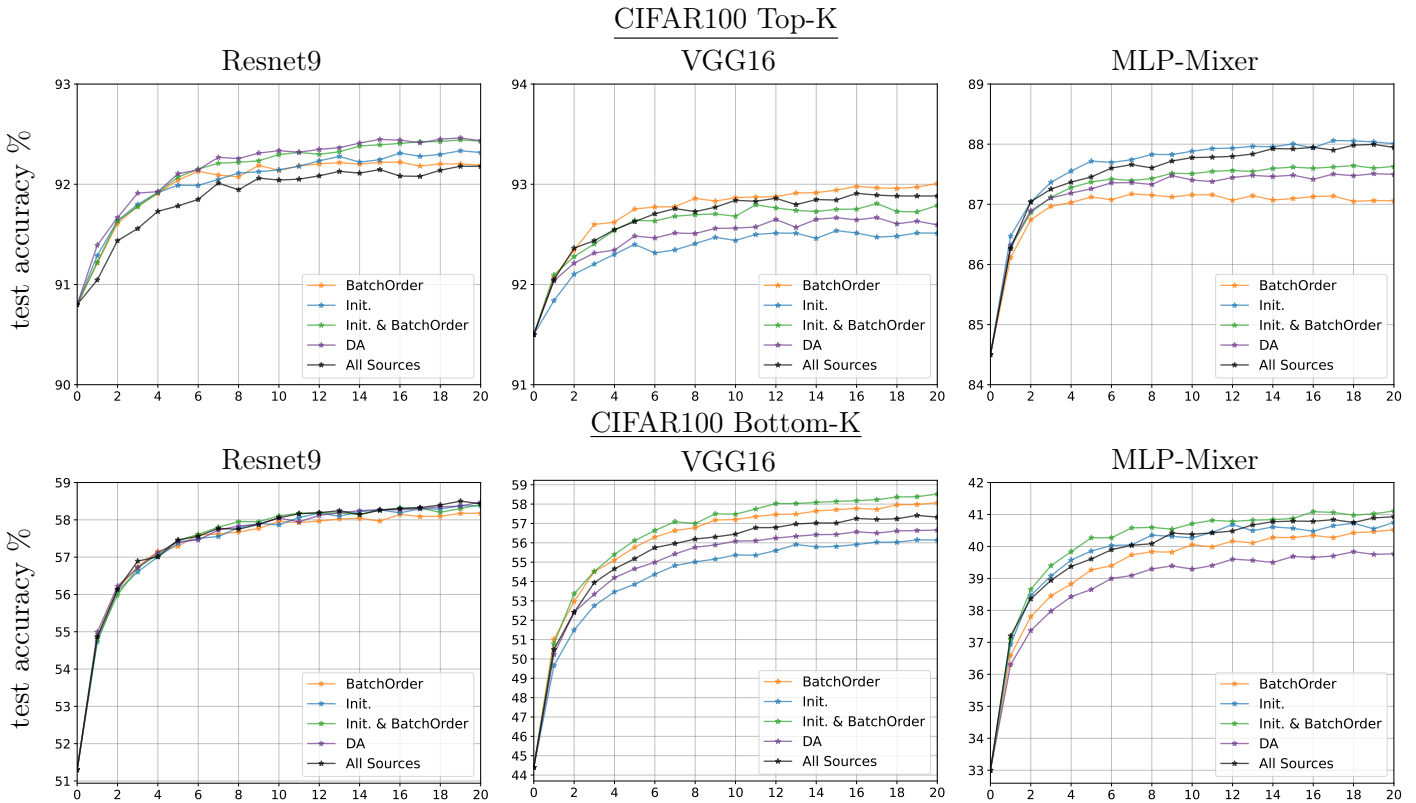
Resnets We train 3 different architectures from the Resnet family (Resnet18, 34, 50) for 100 steps using Stochastic Gradient Descent (SGD). We implemented standard data augmentation by applying Random Resized Crop and Random Horizontal Flip. We use a Slanted Triangular Learning Rate (SLTR) (Howard & Ruder, 2018). The top-1 test set accuracy for Resnet-18 is 49.27%, Resnet-34 is 52.18%, and Resnet-50 is 54.99%

VGG16 We train the model for 100 steps using Stochastic Gradient Descent (SGD). We implemented standard data augmentation by applying Random Resized Crop and Random Horizontal Flip. We use a Slanted Triangular Learning Rate (SLTR) (Howard & Ruder, 2018). The top-1 test set accuracy is 60.37%

ViT We train the model for 100 steps using Adaptive Moment Estimation with decoupled weight decay (AdamW) (Loshchilov & Hutter, 2017). We implemented standard data augmentation by applying Random Horizontal Flip, Random Resized Crop, AutoAugment (Cubuk et al., 2018), Random Erasing (Zhong et al., 2020), Cutmix (Yun et al., 2019), and Mixup(Zhang et al., 2017). We use a combination of warmup for first 10 epoch and cosine annealing (Loshchilov & Hutter, 2016) for scheduler. The top-1 test set accuracy is 51.21%

B Why do ensembles disproportionately benefit bottom-k and minority group performance?

B.1 Can Different Sources of Stochasticity Improve Deep Ensemble Fairness?



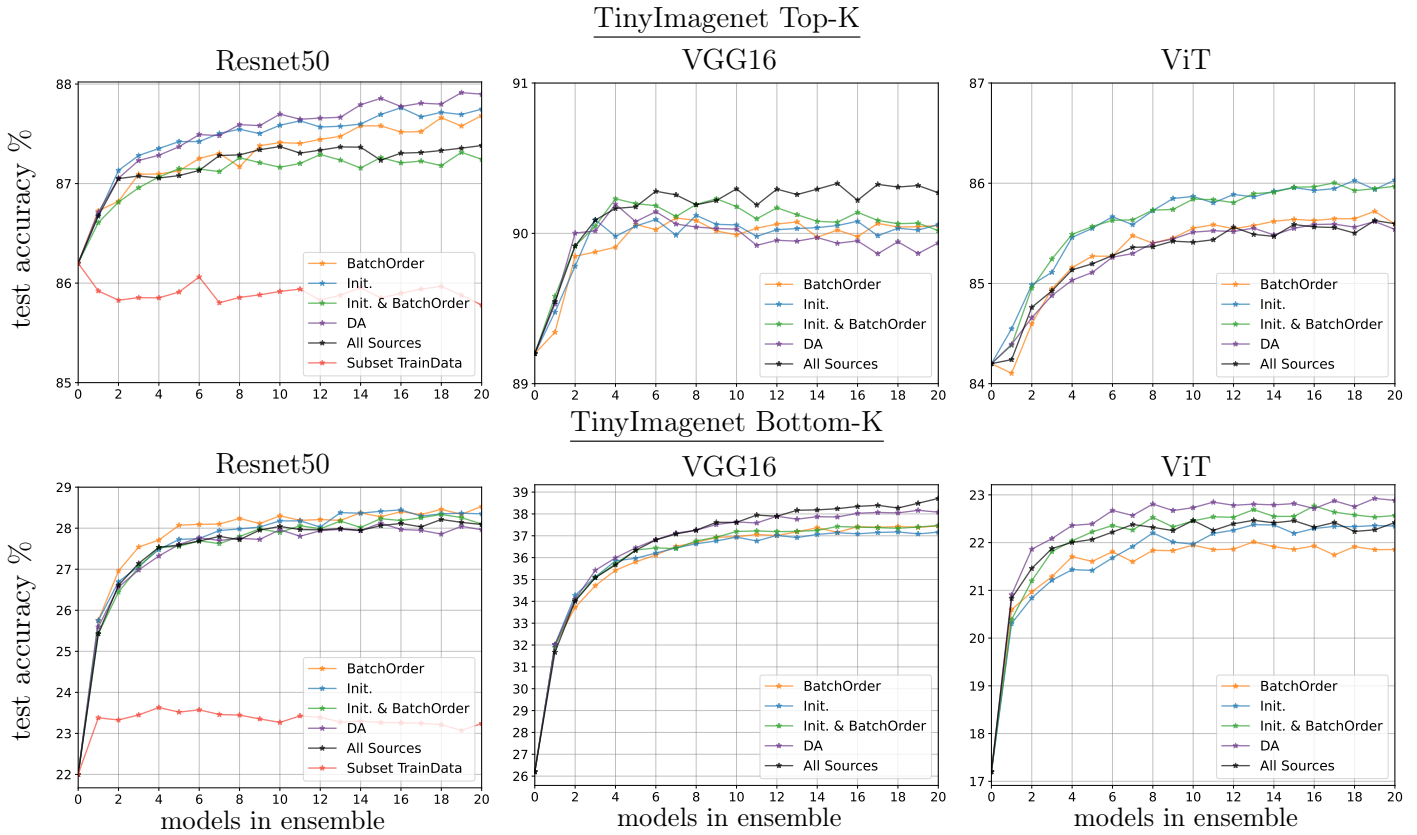


Figure 8: Average Test Accuracy on CIFAR100 and TinyImagenet for Top-K and Bottom-K ($K=10$) Performing Classes

C Experimental Set-up

C.1 Balanced Dataset Sub-Groups

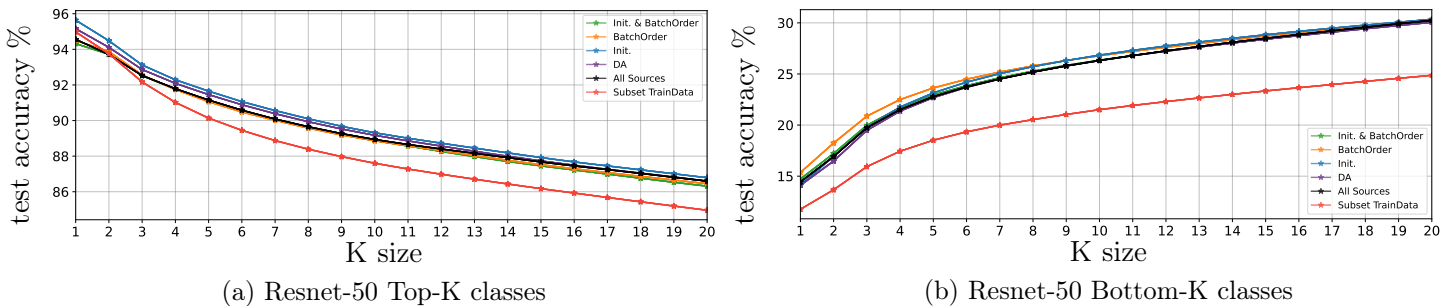


Figure 9: Average Top and Bottom-K accuracy as number of K -classes increase. We observe that **DA** and **Init.** outperforms **All Sources** baseline performance in Top-K classes, whereas **BatchOrder** and **Init.** outperforms **All Sources** on Bottom-K classes. In both top and bottom groups, only the **TrainSubsetData** variant underperforms **All Sources**.

D Can Different Sources of Stochasticity Improve Deep Ensemble Fairness?

D.1 Dominant sources of stochasticity

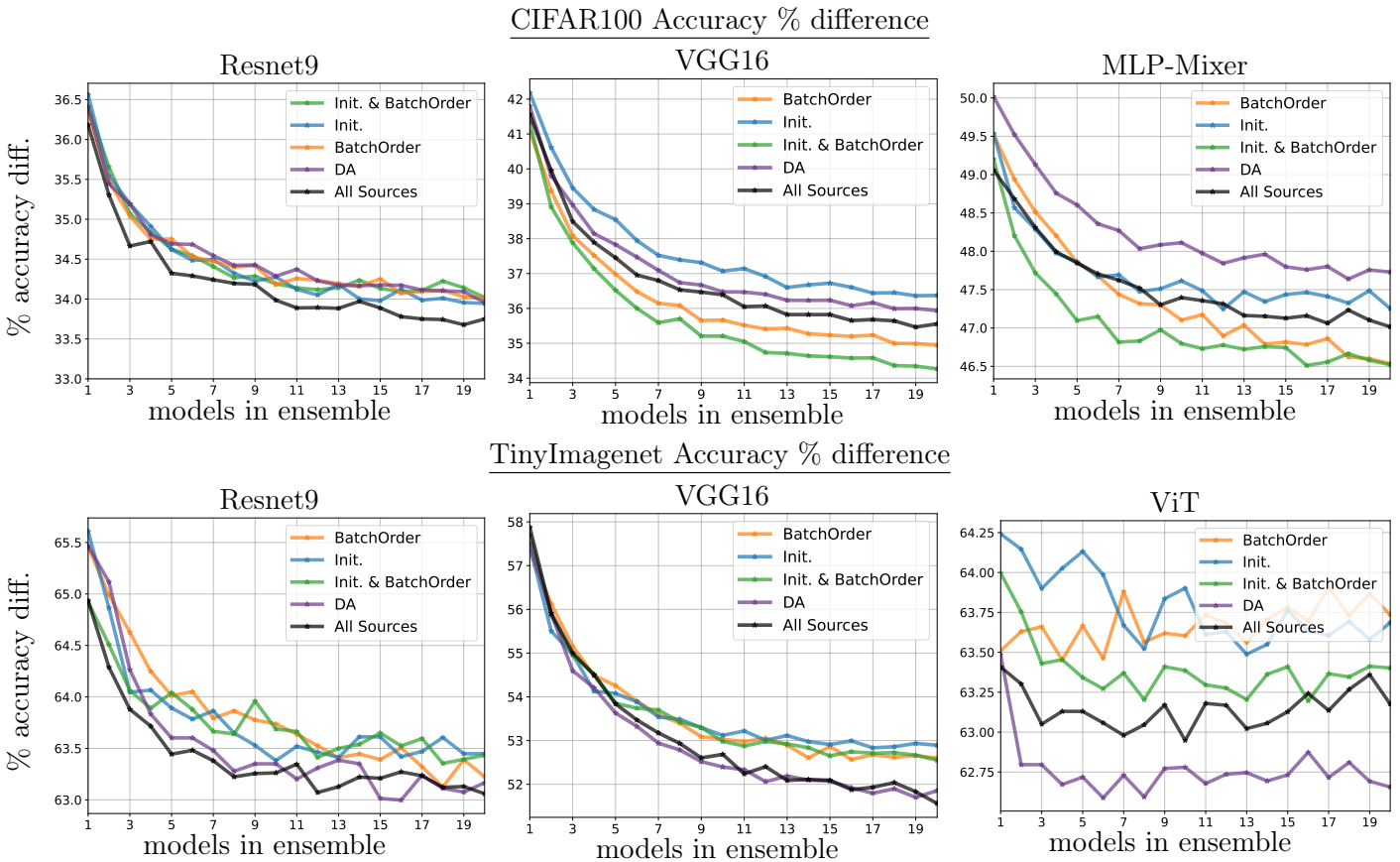


Figure 10: Accuracy % difference between top and bottom 10 classes for Resnet-9, VGG16, and MLP-Mixer trained on CIFAR100 and TinyImagenet

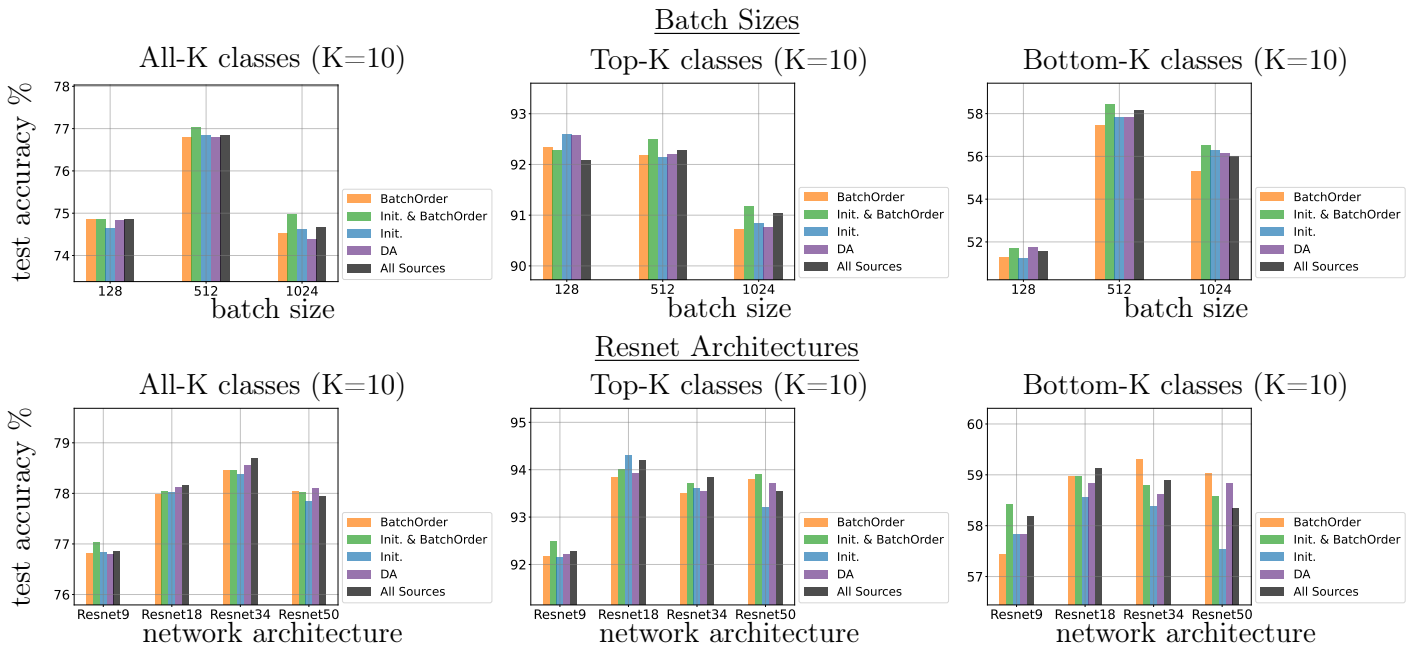


Figure 11: Average Test Accuracy on CIFAR100 as batch and architecture size increases. Batch 512 is default.

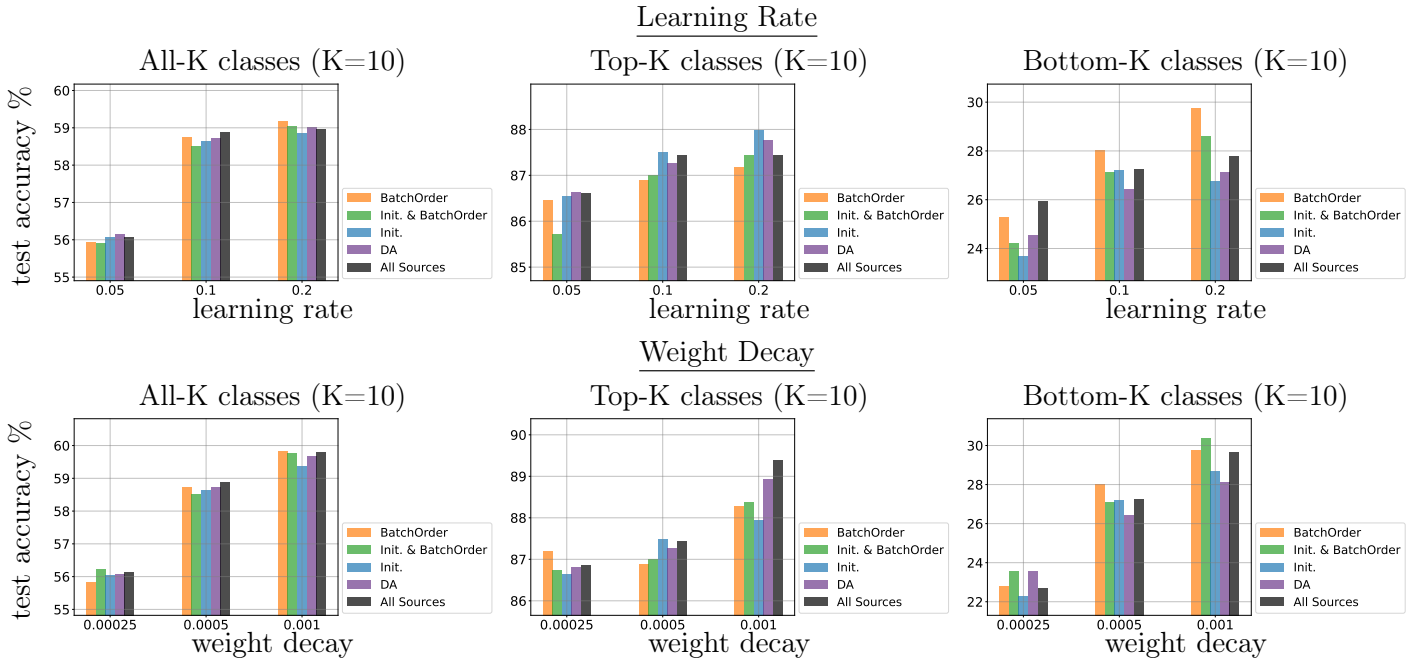


Figure 12: Average Eval Accuracy on TinyImagenet as learning rate and weight decay increases. 0.1 is default learning rate, and 0.0005 is default weight decay.

E Results and Discussion

E.1 Ensembling provides disproportionate gains to bottom-k and minority classes

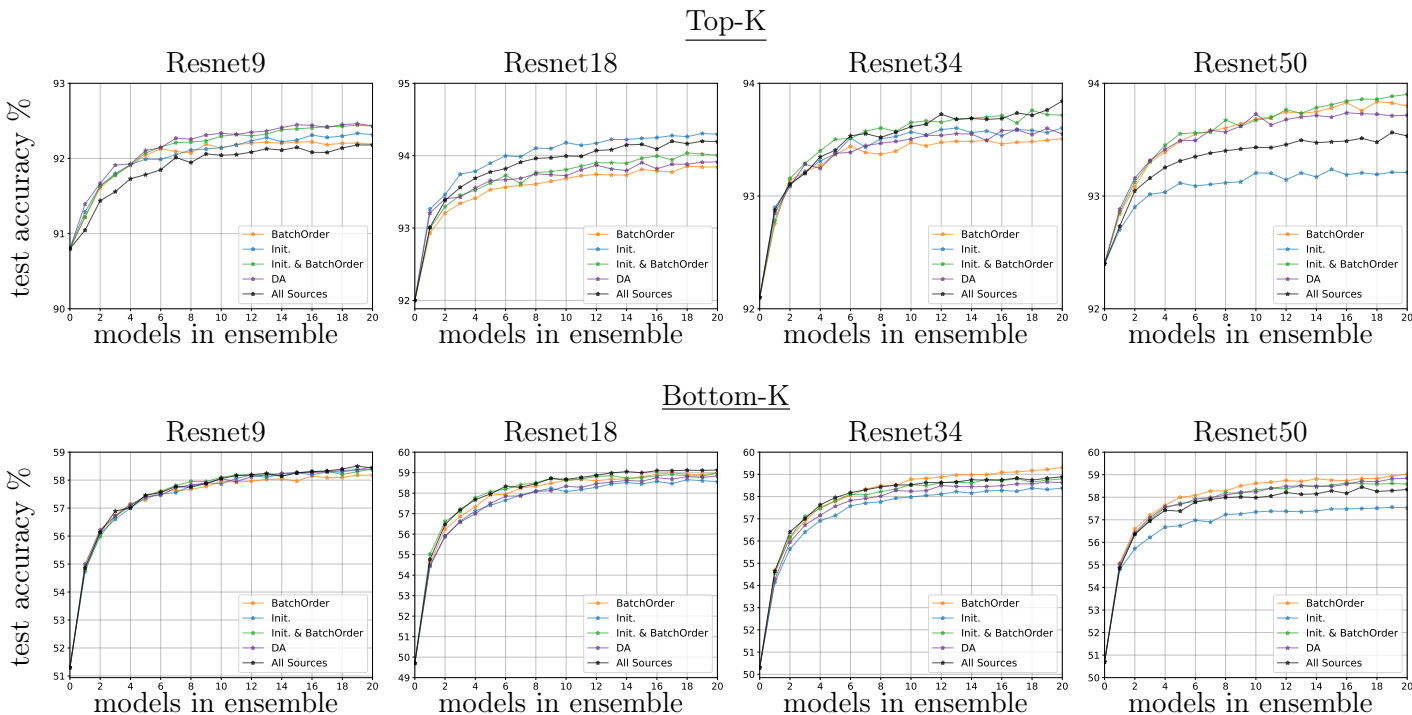


Figure 13: Average Test Accuracy on CIFAR100 for Top-K and Bottom-K classes across different sizes of Resnets.

F Ensembling provides disproportionate gains to bottom-k and minority classes

F.1 Benefits of even larger ensembles

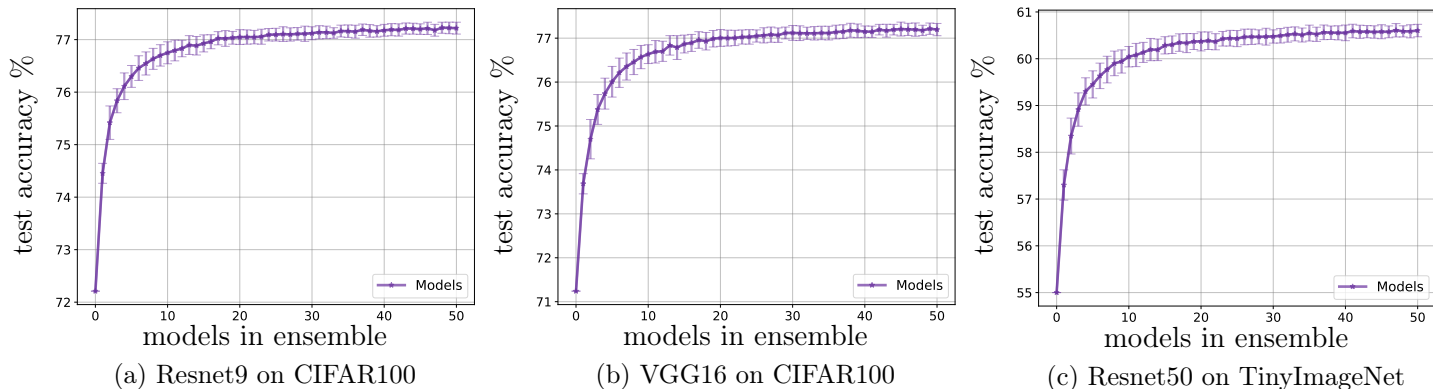


Figure 14: Average Accuracy per size of ensemble. The average accuracy for each model added is calculated by averaging 100 random samples from a population of 50 models. We can see that the average accuracy starts to slowly plateau as the ensemble grows to 50 models.

F.2 CIFAR-100

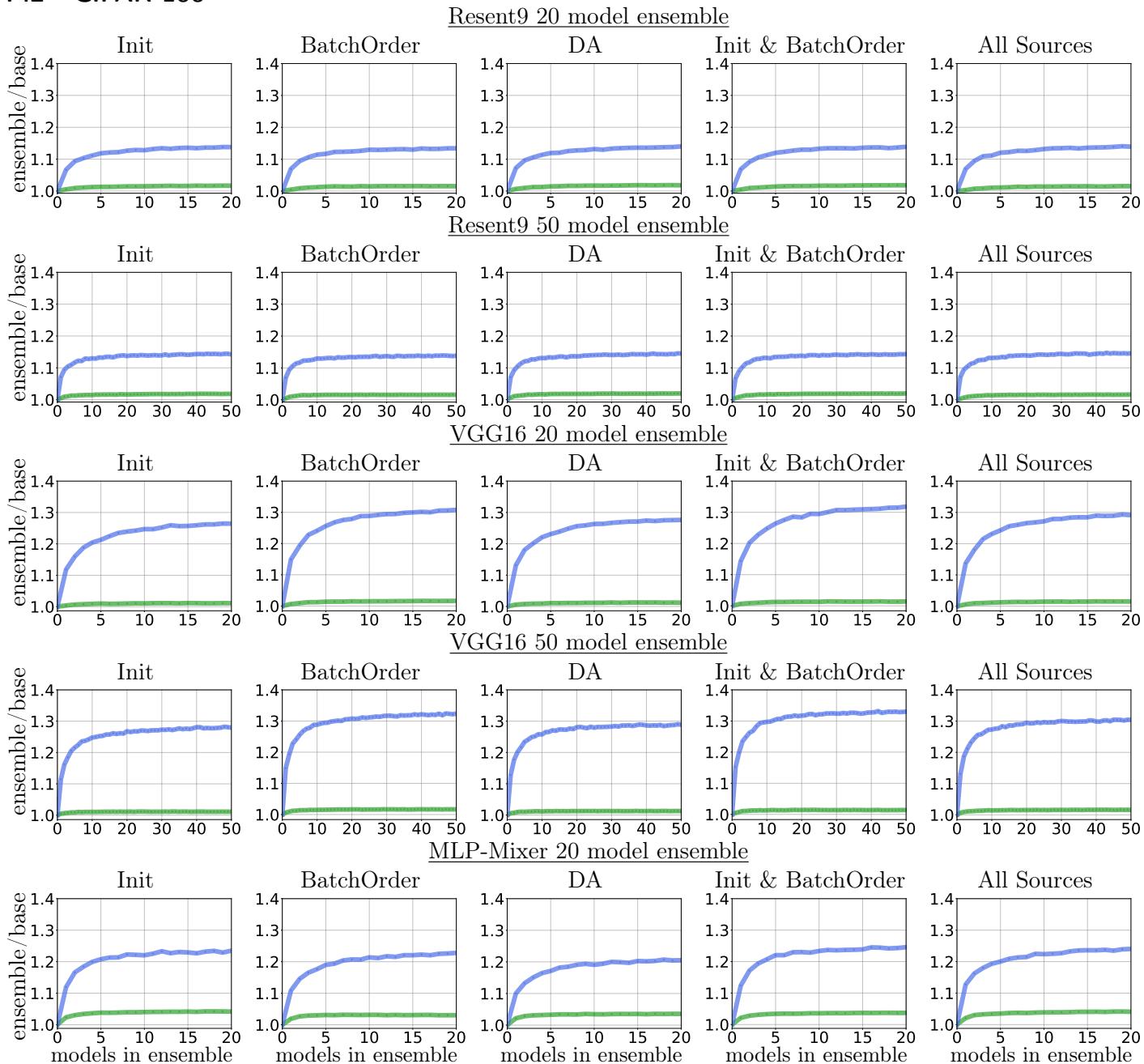
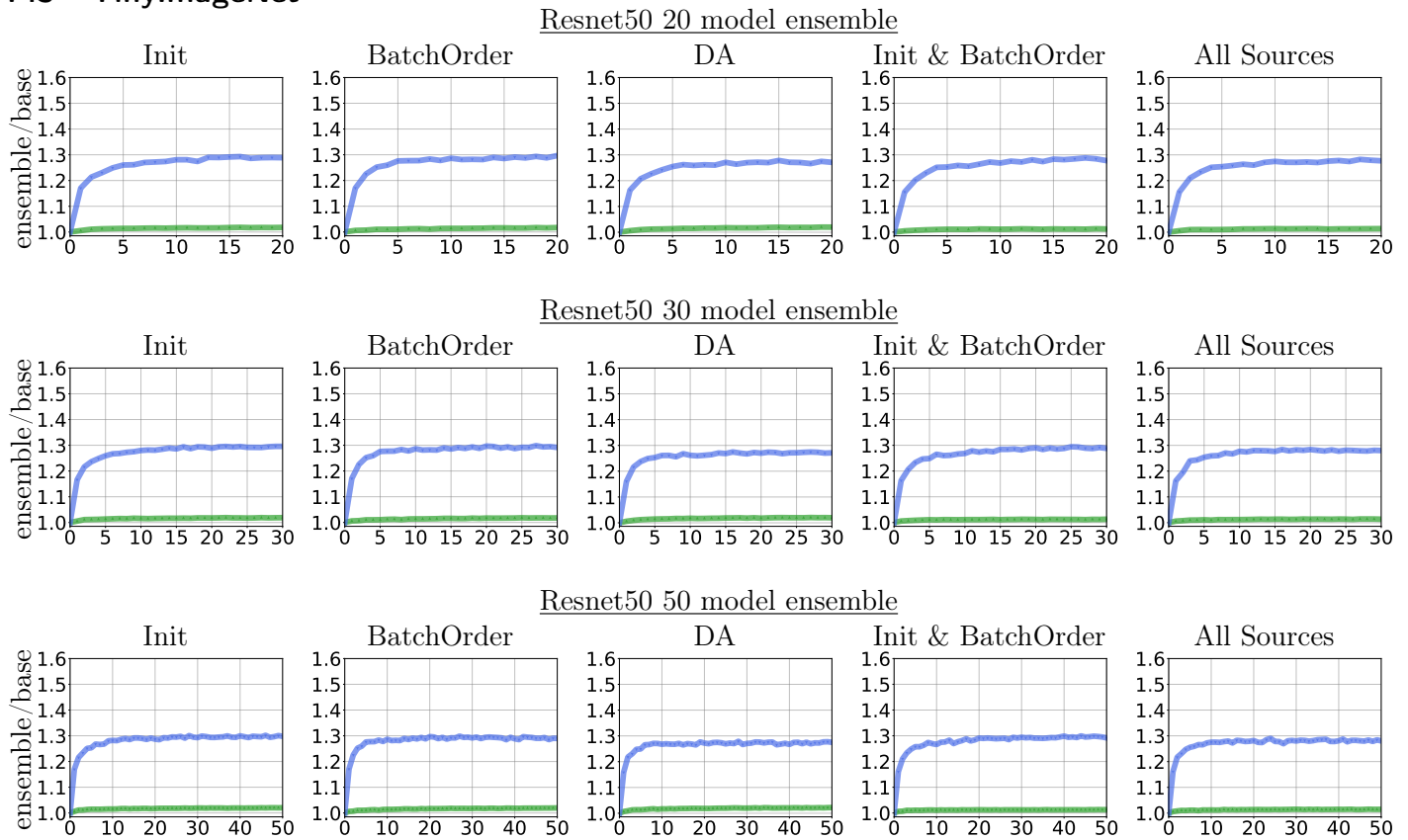


Figure 15: Ratio of Top & Bottom K ensemble accuracy for different model architectures and ensemble sizes on CIFAR100

F.3 TinyImageNet



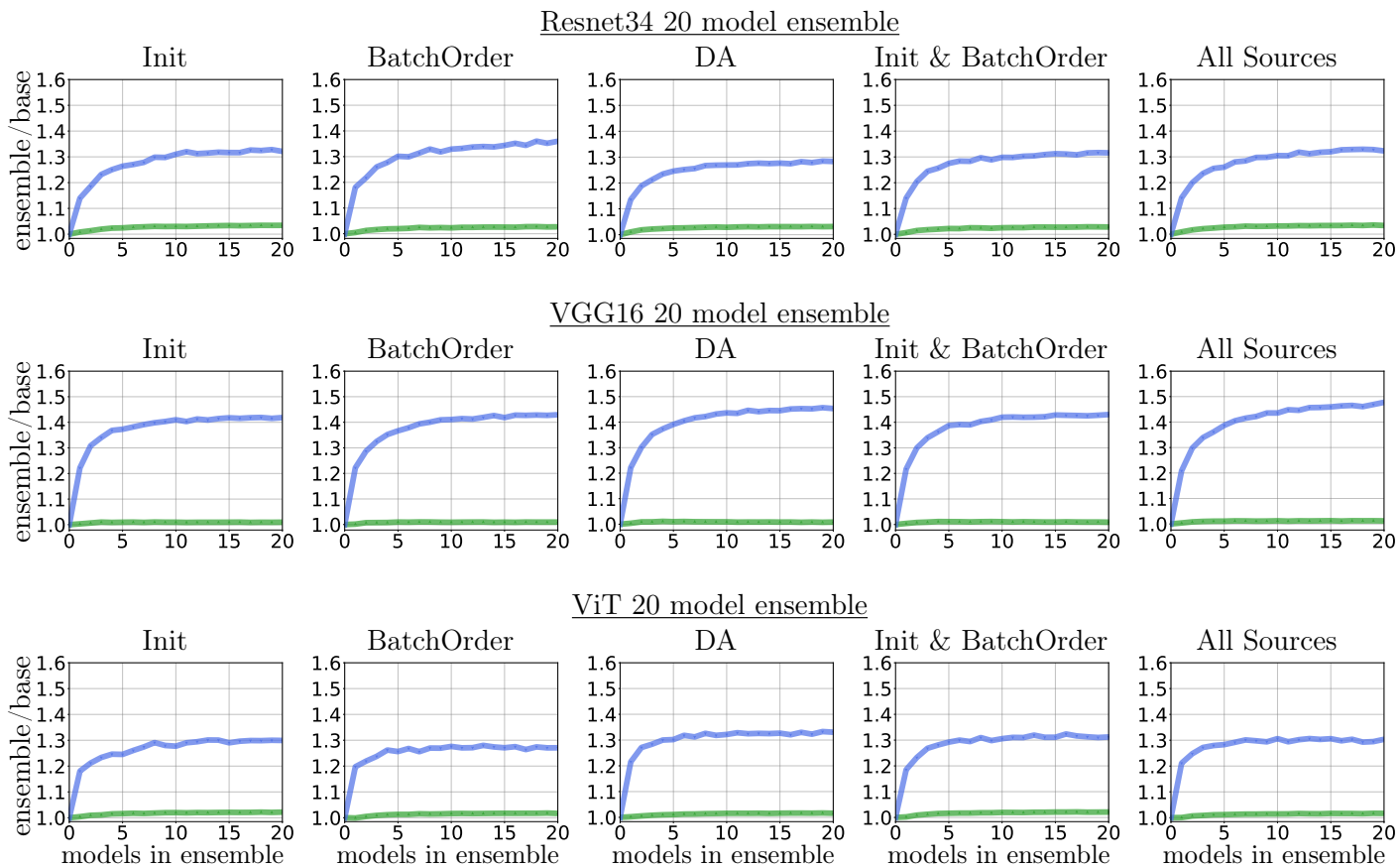


Figure 16: Ratio of Top & Bottom K ensemble accuracy for different model architectures and ensemble sizes on TinyImageNet

G FAIR Ensemble: Improved Robustness

G.1 Data Corruption

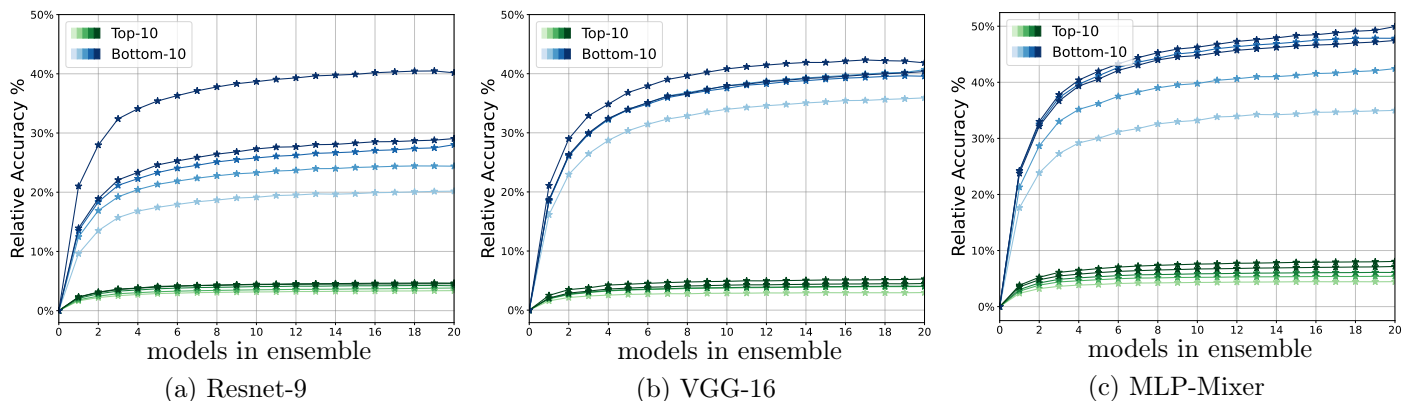


Figure 17: Performance on CIFAR-100 Corrupt based on Severity Levels.

H Results and Discussion

H.1 CIFAR100

Table 3: Top-10 and Bottom-10 class names for CIFAR100. The classes are from the averaged test accuracies from the 20-model ensembles.

| Resnet9 | Resnet18 | Resnet34 | Resnet50 | VGG16 | MLP-Mixer |
|------------|------------|---------------|---------------|------------|------------|
| Top-10 | | | | | |
| wardrobe | skunk | skunk | orange | road | wardrobe |
| motorcycle | orange | road | wardrobe | wardrobe | motorcycle |
| orange | motorcycle | orange | motorcycle | sunflower | orange |
| skunk | road | sunflower | skunk | motorcycle | sunflower |
| road | wardrobe | motorcycle | road | skyscraper | road |
| chimpanzee | palm_tree | wardrobe | sunflower | skunk | skyscraper |
| sunflower | chimpanzee | palm_tree | chimpanzee | palm_tree | keyboard |
| orchid | sunflower | pickup_truck | palm_tree | orange | palm_tree |
| mountain | tractor | aquarium_fish | aquarium_fish | chair | plain |
| apple | skyscraper | skyscraper | lawn_mower | chimpanzee | skunk |
| Bottom-10 | | | | | |
| man | mouse | shark | girl | possum | mouse |
| shark | bear | possum | lizard | crocodile | bowl |
| lizard | shark | crocodile | possum | girl | woman |
| bowl | girl | lizard | maple_tree | shark | girl |
| possum | lizard | girl | bear | bear | squirrel |
| shrew | man | man | otter | lizard | possum |
| seal | otter | bowl | bowl | seal | lizard |
| girl | seal | otter | man | boy | boy |
| otter | bowl | seal | boy | otter | otter |
| boy | boy | boy | seal | man | seal |

H.2 TinyImageNet

Table 4: Top-10 and Bottom-10 wnid names for TinyImagenet. The names are from the averaged test accuracies from the 20-model ensembles.

| Resnet9 | Resnet18 | Resnet34 | Resnet50 | VGG16 | ViT |
|-----------|-----------|-----------|-----------|-----------|-----------|
| Top-10 | | | | | |
| n02791270 | n02791270 | n02791270 | n02791270 | n02791270 | n07875152 |
| n02509815 | n02509815 | n02509815 | n02509815 | n03042490 | n03814639 |
| n03976657 | n02906734 | n02906734 | n02906734 | n02509815 | n03983396 |
| n02124075 | n03042490 | n03814639 | n03042490 | n03814639 | n03042490 |
| n03814639 | n03814639 | n01950731 | n01950731 | n02906734 | n02823428 |
| n03089624 | n03976657 | n03599486 | n04067472 | n01950731 | n03599486 |
| n03983396 | n01950731 | n03042490 | n03599486 | n04398044 | n02509815 |
| n02002724 | n04560804 | n03976657 | n03976657 | n02124075 | n02791270 |
| n03126707 | n03599486 | n04067472 | n07579787 | n03089624 | n03126707 |
| n03447447 | n02002724 | n03126707 | n03126707 | n04067472 | n02906734 |
| Bottom-10 | | | | | |
| n02437312 | n04532670 | n03160309 | n03544143 | n02085620 | n02927161 |
| n04070727 | n03544143 | n01945685 | n03617480 | n04417672 | n03544143 |
| n02268443 | n04486054 | n04417672 | n04070727 | n02268443 | n04070727 |
| n01945685 | n02268443 | n04532670 | n03804744 | n04486054 | n01641577 |
| n02226429 | n03160309 | n03617480 | n03160309 | n01945685 | n02094433 |
| n02233338 | n03617480 | n01855672 | n01945685 | n02094433 | n02480495 |
| n02480495 | n01855672 | n03804744 | n02268443 | n04070727 | n02410509 |
| n02410509 | n02480495 | n02480495 | n02480495 | n02480495 | n04532670 |
| n03617480 | n02123394 | n02123394 | n02123394 | n02410509 | n02950826 |
| n02123394 | n02410509 | n02410509 | n02410509 | n02123394 | n02123394 |